Metabolism of Trichloroethylene

Lawrence H. Lash,[1] Jeffrey W. Fisher,[2] John C. Lipscomb,[3] and Jean C. Parker[4]

[1]Department of Pharmacology, Wayne State University School of Medicine, Detroit, Michigan USA; [2]Toxicology Division, Armstrong Laboratory, Wright-Patterson AFB, Ohio USA; [3]National Center for Environmental Assessment, U.S. Environmental Protection Agency, Cincinnati, Ohio USA; [4]National Center for Environmental Assessment, U.S. Environmental Protection Agency, Washington, DC USA

A major focus in the study of metabolism and disposition of trichloroethylene (TCE) is to identify metabolites that can be used reliably to assess flux through the various pathways of TCE metabolism and to identify those metabolites that are causally associated with toxic responses. Another important issue involves delineation of sex- and species-dependent differences in biotransformation pathways. Defining these differences can play an important role in the utility of laboratory animal data for understanding the pharmacokinetics and pharmacodynamics of TCE in humans. Sex-, species-, and strain-dependent differences in absorption and distribution of TCE may play some role in explaining differences in metabolism and susceptibility to toxicity from TCE exposure. The majority of differences in susceptibility, however, are likely due to sex-, species-, and strain-dependent differences in activities of the various enzymes that can metabolize TCE and its subsequent metabolites. An additional factor that plays a role in human health risk assessment for TCE is the high degree of variability in the activity of certain enzymes. TCE undergoes metabolism by two major pathways, cytochrome P450 (P450)-dependent oxidation and conjugation with glutathione (GSH). Key P450-derived metabolites of TCE that have been associated with specific target organs, such as the liver and lungs, include chloral hydrate, trichloroacetate, and dichloroacetate. Metabolites derived from the GSH conjugate of TCE, in contrast, have been associated with the kidney as a target organ. Specifically, metabolism of the cysteine conjugate of TCE by the cysteine conjugate β-lyase generates a reactive metabolite that is nephrotoxic and may be nephrocarcinogenic. Although the P450 pathway is a higher activity and higher affinity pathway than the GSH conjugation pathway, one should not automatically conclude that the latter pathway is only important at very high doses. A synthesis of this information is then presented to assess how experimental data, from either animals or from *in vitro* studies, can be extrapolated to humans for risk assessment. *Key words*: conjugate beta-lyase, cysteine glutathione, cytochrome P450, glutathione *S*-transferases, metabolism, sex dependence, species dependence, tissue dependence, trichloroethylene. — *Environ Health Perspect* 108(suppl 2):177–200 (2000).
http://ehpnet1.niehs.nih.gov/docs/2000/suppl-2/177-200lash/abstract.html

An understanding of the importance of each pathway of trichloroethylene (TCE) metabolism is critical for determining susceptibility, target organ specificity, and extrapolation of animal data to humans. Both a qualitative and a quantitative understanding of sex and species differences in metabolism should allow more accurate physiologically based pharmacokinetic (PBPK) modeling to be done and, hence, more accurate risk assessments to be made. Of course, the ability to obtain some metabolism data from human tissue enables comparison of modeling data with actual data and assessment of the accuracy of the PBPK models. The final section of the review highlights some of the principal remaining questions and research needs relating to metabolism of TCE.

A scheme summarizing the major metabolic pathways for TCE is shown (Figure 1). As described below and in other reviews in this monograph, the metabolic flux through the oxidative and glutathione (GSH)-dependent pathways differ in each tissue. Hence, modes of action for each target organ, which are largely dependent on the chemical species generated, will differ. Most of the focus on the oxidative pathway has been on the liver, which has the highest activities of any tissue of the various isoforms of cytochrome P450 (P450). P450-derived metabolites have been directly associated with liver injury. The lungs are additional target organs for which P450-derived metabolites have been linked to toxic and pathologic processes. Although P450 activity is present in the kidneys, to date the nephrotoxic and potential nephrocarcinogenic effects of TCE have only been associated with metabolites derived from the GSH conjugation pathway. As described in subsequent sections of this review, the reactions of the GSH conjugation pathway, with the exception of the initial conjugation step, which occurs predominantly in the liver but can also occur in extrahepatic tissues, occur in the kidneys. This is caused by tissue-selective localization of transport processes and bioactivation steps (i.e., the cysteine conjugate β-lyase [β-lyase]) in epithelial cells of the renal proximal tubules.

For the ultimate purpose of human health risk assessment, it is important to put the metabolism data in the context of actual, potential exposures. Hence, for most environmental exposures to TCE, such as those that may occur with contaminated drinking water, rates of metabolism in humans may be extremely small because of high K_m and low V_{max} values relative to those found in rodents. At higher occupational exposures to TCE, however, many of these metabolic pathways may be quantitatively significant in humans as well. A discussion of exposure levels in the human population is beyond the scope of this review. Readers are referred to the review by Wu et al. (*1*) on TCE exposure assessment and the review on PBPK modeling by Clewell et al. (*2*) in this monograph for more detailed discussions of exposures that are relevant to humans.

In Vivo Absorption and Distribution of TCE

As a result of its chemical properties (e.g., volatility, lipophilicity), TCE is readily absorbed across biological membranes. For human exposures, TCE is considered to be an eye and skin irritant. There are essentially three types of exposures to consider for humans or laboratory animals: inhalation, dermal, and oral. Exposure is usually either from TCE vapor or from TCE liquid. In either form, TCE is rapidly and extensively absorbed through the lungs or gastrointestinal tract, respectively. Absorbed TCE is then subsequently distributed to different target organs (e.g., lungs, liver, kidneys, nervous system) via the circulatory system.

After inhalation exposure, TCE is rapidly and extensively absorbed through the alveolar endothelium due to a high blood/gas partition coefficient. Although absorption is high in all cases, blood/gas partition coefficients vary significantly among species (Table 1). Since the blood/gas partition coefficient in humans is approximately 1.5- and 2.5-fold lower than that in mice and rats, respectively,

This article is part of the monograph on Trichloroethylene Toxicity.

Address correspondence to L.H. Lash, Dept. of Pharmacology, Wayne State University School of Medicine, 540 East Canfield Ave., Detroit, MI 48201. Telephone: (313) 577-0475. Fax: (313) 577-6739. E-mail: l.h.lash@wayne.edu

The views expressed in this article are those of the authors and do not necessarily reflect the views or policies of the U.S. government agencies.

Received 20 October 1999; accepted 21 January 2000.

this suggests that delivery of TCE to the circulatory system for translocation to target organs may be significantly less efficient in humans than in rodents and is a factor that may need to be taken into account when using animal data in a risk assessment analysis for TCE.

Dermal absorption from exposure to TCE vapor is negligible, although direct skin contact with TCE liquid may lead to significant absorption. Since a large proportion of the TCE that is absorbed dermally in humans is excreted unchanged through the lungs and this is not the usual route of exposure to TCE, dermal absorption is not considered to be a major factor in the risk assessment analysis (*3*). These data have been reviewed by Davidson and Beliles (*4*). It should be noted, however, that a study of dermal absorption of dilute, aqueous solutions of TCE and similar organic solvents in hairless guinea pigs indicated that significant absorption occurs (*5*). This type of exposure mimics that of the human population to drinking water contaminated with TCE. Hence, dermal absorption should be considered in risk assessment analyses for this type of exposure.

Besides inhalation, oral absorption is a major factor in exposure to TCE. Since TCE is uncharged, nonpolar, and highly lipophilic, gastrointestinal absorption is extensive and occurs by passive diffusion. One would expect, therefore, that oral absorption would be a nonvarying element in the pharmacokinetics of TCE. However, differences in oral absorption of TCE are evident when TCE is administered either in water or corn oil. For example, Withey et al. (*6*) demonstrated that peak blood concentrations of TCE in rats given an intragastric dose (18 mg/kg) in water was nearly 15-fold higher than those in rats given the same dose in the same volume of corn oil (14.7 vs 1.0 µg/mL). Hence, the authors concluded that gastrointestinal absorption of TCE can be limited by the absorption of the vehicle. The vehicle used in exposures in animal studies, therefore, needs to be taken into account when extrapolating animal exposure data for human health risk assessment.

As a consequence of differences in blood flow and overall metabolic rate, species differences exist in the fraction of administered dose of TCE that is available for conversion to toxic metabolites in the target organs. For example, Prout et al. (*7*) compared blood concentrations of TCE, chloral hydrate (CH), trichloroethanol (TCOH), and trichloroacetate (TCA) over time after administration of a 1,000 mg/kg oral dose of TCE to male Osborne-Mendel rats and male B6C3F$_1$ mice. They observed that blood concentrations for the three metabolites of TCE were markedly higher in mice than in rats at most time points, whereas those for TCE were higher in rats than in mice, indicating more rapid metabolism and elimination of TCE in the mice (Table 2). Furthermore, the area under the curve (AUC) was severalfold higher for CH, TCOH, and TCA in mice than in rats. Fisher et al. (*8*) also observed approximately 5-fold higher peak blood concentrations of TCE in male and female rats compared with male and female mice and

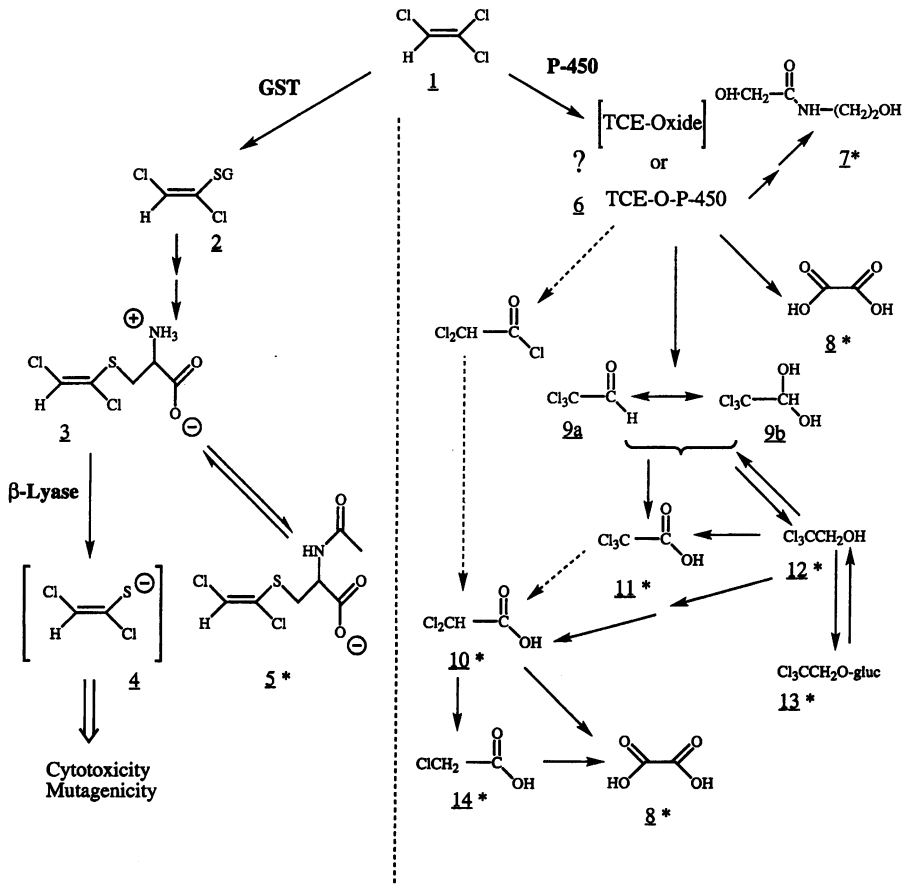

Figure 1. Scheme of metabolism of TCE. Metabolites marked with an asterisk are known urinary metabolites. Metabolites: 1 = TCE; 2 = DCVG; 3 = DCVC; 4 = 1,2-dichlorovinylthiol; 5 = NAcDCVC; 6 = TCE-P450 or TCE-oxide intermediate; 7 = *N*-(hydroxyacetyl)-aminoethanol; 8 = oxalic acid; 9a = chloral; 9b, chloral hydrate; 10 = dichloroacetic acid; 11 = trichloroacetic acid; 12 = trichloroethanol; 13 = trichloroethanol glucuronide; 14, monochloroacetic acid.

Table 1. Reported blood/gas coefficient for TCE in rats, mice, and humans.

Species	Blood/gas coefficient	Reference
Rat		
F344, male	25.8	(*163*)
SD, male	21.9	(*8*)
F344, male	21.9	(*7*)
F344, female	15.0	(*7*)
Mouse		
B6C3F$_1$, male	13.4	(*7*)
B6C3F$_1$, female	14.3	(*7*)
Human, both male	9.92	(*163*)
	9.2	(*164*)

SD, Sprague-Dawley.

Table 2. Blood concentrations of TCE and selected metabolites in male Osborne-Mendel rats and male B6C3F$_1$ mice after an oral dose of TCE.[a]

	Peak blood concentration (µg/mL)	Time after exposure of peak (hr)	AUC (mice:rats)
TCE			
Rats	61.4	3.0	
Mice	18.2	0.5	
			7.9
CH			
Rats	0.86	9.0	
Mice	1.77	3.0	
			1.0
TCOH			
Rats	8.0	10.0	
Mice	33.5	2.0	
			3.9
TCA			
Rats	50	14.0	
Mice	263	14.0	
	288	30.0	
			6.3

[a]Rats and mice were given TCE (1,000 mg/kg) per os in corn oil. Blood samples were taken by cardiac puncture and were analyzed by gas chromatography. AUC were determined graphically up to the final time point taken (TCE: 7.5 hr in rats, 11 hr in mice; CH: 15 hr in rats, 10 hr in mice; TCOH: 18 hr in rats, 8 hr in mice; TCA: 40 hr in rats, 44 hr in mice). For TCA in mice, two major peaks of blood concentration were observed. Data originally reported in Prout et al. (*7*).

similarly higher peak plasma concentrations of TCA in male and female mice compared with male and female rats. These observations have important implications for species differences in susceptibility to toxicity. As discussed in the review on mode of action in the liver (*9*), TCA is believed to be the primary TCE metabolite responsible for liver injury and proliferation. The markedly higher blood concentrations of TCA in mice compared with rats indicate that more TCA will get to the target organ in mice and are consistent with the male mouse as the sex and species that is the most susceptible to liver injury and carcinogenesis.

In analyzing the distribution of TCE into various tissues, three major compartmental tissue groups can be identified: richly perfused (e.g., liver, kidneys, lung), poorly perfused (e.g., muscle), and adipose tissue. TCE readily equilibrates from the circulation into richly perfused tissues, with reported partition coefficients for liver:blood or richly perfused tissue:blood for male rats of approximately 1.2 (*8,10*). Partition coefficients for female rats (1.46) and for male and female mice (2.03 and 1.62, respectively) are modestly higher than those in male rats (*8*), but these modest differences are not likely to be major factors in the sex- and species-dependent differences in TCE-induced toxicity. Muscle:blood partition coefficients for TCE have been reported to be less than 0.5 for male and female rats and female mice and 1.00 for male mice (*8,10*). Hence, muscle is neither a major site of storage nor a major site of metabolism of TCE and does not significantly influence TCE pharmacokinetics or pharmacodynamics.

Although the adipose tissue:blood partition coefficient does not differ greatly among male and female rats and mice, with reported values ranging between 25 and 41 (*8*), the fact that it is so high indicates that sequestration of TCE in fat may have a major influence on the pharmacokinetics of TCE. In fact, the half-life of TCE in adipose tissue is estimated to be 3.5–5 hr, whereas that in both the richly and poorly perfused compartments is estimated to be 2–4 min (*4*). Hence, slow release of TCE from fat several hours after initial exposures to TCE can lead to continued delivery of TCE to target organs. Fat may also be a site of metabolism of TCE, as cytochrome P4502E1 (CYP2E1) is present in adipose tissue microsomes (*11*).

Pharmacokinetics of TCE and Its Major Oxidative Metabolites

As described above, orally administered TCE is rapidly and extensively absorbed into the systemic circulation. Daniel (*12*) dosed rats by stomach tube (60 mg/kg) with labeled TCE and reported that 90–95% of the radiolabel was recovered in expired air and urine. Dekant et al. (*13*) gavage-dosed mice and rats with 200 mg/kg of labeled TCE in corn oil and recovered 93–98% of the radiolabel. Prout et al. (*7*) administered several doses of labeled TCE (10–2,000 mg/kg) to rats and mice and recovered 93–98% of the radiolabel and reported that peak blood levels occurred in 1 hr in mice and 3 hr in rats. D'Souza et al. (*14*), using classical pharmacokinetic analysis, reported that oral and intravenous bioavailability of TCE was 60–90% in nonfasted rats and greater than 90% in fasted rats. Peak blood levels occurred between 6–10 min and blood concentrations were 2–3 times higher in the fasted rats compared with the nonfasted rats. Lee et al. (*15*) empirically demonstrated that presystemic elimination (metabolism) of low dose rates of TCE was inversely related to dose and was nonlinear, leading these authors to suggest that trace amounts of TCE in the drinking water may not enter the systemic circulation.

No controlled oral ingestion studies in human have been reported in the literature for TCE. Evidence for oral uptake of TCE in humans is inferred from case studies that report poisonings. Accidental or intentional ingestion of large amounts of TCE has occurred, resulting in death (*16*). A more recent study of an attempted suicide of a 17-year old who ingested 70 mL of TCE also shows rapid systemic uptake and tissue distribution, with peak blood concentrations of TCE being obtained 13 hr after ingestion (*17*).

Inhalation of TCE results in very rapid uptake of TCE into the systemic circulation in animals (*8*) and humans (*18*), although the time required to reach peak blood concentrations differs across species. Peak blood concentrations of TCE are achieved within 1–2 hr in mice exposed to 100–750 ppm TCE vapors, in 4–6 hr in rats exposed to 500–600 ppm TCE vapors, and in 8–12 hr in humans exposed to 100 ppm TCE.

Once TCE is in the systemic circulation, TCE is oxidized (metabolized) rapidly. Using PBPK models, estimates of metabolic capacity have been determined in rodents and humans, and are summarized in Table 3. It is clear that rodents have a much high capacity to metabolize TCE than humans. Estimated values for Michaelis-Menten affinity constants (K_m) were estimated to be low for rodents and humans (0.25–1.5 mg/L), reflecting a high substrate (TCE) affinity.

Although several metabolic products derived from the GSH and P450 metabolic pathways have been identified for TCE, only a few of the major metabolites have been characterized pharmacokinetically in rodents and humans. The plasma half-life of TCA in humans ranges from 86 to 99 hr after inhalation of either 50 or 100 ppm TCE, 6 hr/day for either 5 or 10 days (*19*). Oral administration of either TCOH (10 mg/kg) or CH (15 mg/kg) in humans resulted in a 63- to 65-hr plasma half-life for the metabolite, TCA. Administration of TCA alone (3 mg/kg) resulted in a plasma half-life for TCA of 51 hr (*19*).

The plasma half-life values for TCA are much shorter in rodents than in humans. In rats given intravenous administration of TCA (5–6 mg/kg), the TCA plasma half-lives were 12 and 7 hr in males and females, respectively (*8*). In mice given intraperitoneal doses of TCA (5–10 mg/kg), the plasma half-lives for TCA were 7 and 3 hr for males and females, respectively (*8*). In mice exposed to TCE vapors (42–889 ppm) for 4 hr, the estimated plasma half-life values for TCA were 16 and 7 hr for males and females, respectively (*8*). In male and female rats exposed to TCE vapors (500–600 ppm), the estimated half-life value for TCA in plasma was 15 hr (*20*).

The residence time for free TCOH in blood is less than the residence time in plasma for TCA in rodents and humans. The half-life of free TCOH in blood is about 12 hr in humans exposed to 50 ppm TCE vapors 6 hr per day for 5 days (*21*) and is 3 hr in mice administered 1,200 mg/kg TCE via oral bolus intubation (*22*). Two other oxidative end products readily found in blood of mice administered TCE that are not readily measured in human blood are chloral hydrate and trichloroethanol glucuronide. CH and TCOH glucuronide (TCOG) were not measured in humans exposed to 100 ppm TCE for 4 hr (*19*). In mice gavage-dosed with 1,200 mg/kg of TCE, the blood half-life values for CH and TCOG were 3 and 5 hr, respectively (*22*).

Oxidative Pathways of TCE Metabolism

This section describes each step of the oxidative pathway of TCE metabolism and identifies key metabolites that are thought to be important for development of toxicity or carcinogenesis. Although many of the enzymes

Table 3. Species-dependent differences in metabolic capacity for TCE.[a]

Species	Metabolic capacity ($V_{max}C$)	Reference
Humans	14.9 4–5	(*15*) (*16*)
Female mice	23.1	(*6,17*)
Male mice	32.7	(*6,17*)
Male and female rats	11–11.5	(*6,17*)

[a]Metabolic capacity ($V_{max}C$) is defined as the maximal rate of metabolism, with units of milligram substrate metabolized per kilogram body weight per hour.

that catalyze the specific steps of this pathway are distributed fairly ubiquitously, a range of activity levels of specific isozymes is found in the different target tissues or in a given tissue in males and females from various species, which can markedly alter the distribution of metabolites that are formed. This, in turn, may have mechanistic implications as tissue- and/or sex- and/or species-specific accumulation of certain metabolites can produce toxic responses that are not otherwise observed.

Description of Oxidative Pathways of TCE Metabolism

Role of formation of TCE-epoxide in oxidative metabolism of TCE. Although TCE is a chemically simple compound, its metabolism is rather complex. The initial step in TCE metabolism, as described above (Figure 1), is either conjugation with GSH (discussed below) or oxidation by P450. The oxidative pathway is quantitatively by far the major pathway for TCE metabolism and the liver is the primary tissue where this step takes place, although P450 isoforms are present in most tissues in varying forms and amounts. The initial step in the oxidative metabolism of many halogenated alkenes is epoxidation (*23*). Hence, the biotransformation of TCE to a reactive epoxide intermediate (2,2,3-trichlorooxirane) was proposed many years ago (*24,25*). The finding of CH as a metabolite of TCE was seen as being consistent with the transient formation of a reactive epoxide intermediate. Epoxides can readily form acyl chlorides, which are subsequently hydrolyzed to the corresponding acids, or they can form aldehydes that are subsequently oxidized to carboxylic acids or reduced to alcohols. The existence of CH, TCOH, and TCA as major metabolites of TCE is in accordance with this scenario. Several years ago, controversy existed over whether TCE oxidation goes through an epoxide intermediate. The significance of this is in the identification of the electrophilic intermediate(s) that can cause cellular injury or mutations. An understanding of the chemical bioactivation mechanism is necessary for elucidating the mode of action of TCE in producing acute cellular toxicity and carcinogenesis.

In spite of the evidence in favor of epoxide formation, Miller and Guengerich (*26,27*) concluded that TCE epoxide is not an obligate intermediate in the formation of CH and that TCE epoxide cannot be the intermediate responsible for irreversible binding to protein and DNA. Although the P450 heme is destroyed during the oxidative metabolism of TCE, the epoxide does not destroy the heme (*27*). Green and Prout (*28*) also concluded that there was little evidence to support the intermediate formation of an epoxide in the oxidative metabolism of TCE in rat or mouse liver microsomes. Furthermore, an epoxide intermediate should yield CO, CO_2, dichloroacetate (DCA), and monochloroacetic acid (CAA) as predominant metabolites from TCE; in contrast to this, CH, TCA, and TCOH are the major oxidative metabolites that are recovered in both *in vivo* and *in vitro* studies (*28*). Miller and Guengerich (*27*) concluded that the species that irreversibly binds to protein and DNA during TCE metabolism must have, unlike an epoxide, a reasonable degree of chemical stability. Hence, the current dogma is that the majority of TCE is believed to undergo chlorine migration in an oxygenated TCE-P450 transition state leading to CH formation. However, Forkert and co-workers (*29–32*) have provided substantial evidence that 1,1-dichloroethylene, which is very similar to TCE, is metabolized by P450 to an epoxide intermediate. These findings suggest that the role of the epoxide in TCE metabolism should be revisited (see discussion under "Questions and Research Needs" below).

The previous conclusion in the last U.S. Environmental Protection Agency risk assessment for TCE (*33*) that an epoxide intermediate is involved in the initial step of the oxidative metabolism of TCE may be erroneous but requires further study. In spite of this, a recent review on TCE metabolism and toxicity (*34*) showed TCE being converted by P450 to CH through an epoxide intermediate and did not consider the oxygenated transition state and chlorine migration. Uncertainty about the significance of an epoxide intermediate still exists, therefore, and needs to be unambiguously resolved.

Metabolism of TCE to chloral hydrate and trichloroethanol. Four different P450 isoforms have been identified as playing a role in TCE metabolism: CYP1A1/2, CYP2B1/2, CYP2C11/6, and CYP2E1 (*35–42*). Of these isoforms, CYP2E1 appears to be the major form with the highest affinity for TCE (*35,36,39*), although considerable variability can exist in the relative roles of different isoforms, depending on physiological state and on the presence of other drugs or inducing agents. Furthermore, as discussed below, most of the work on oxidative metabolism of TCE has been done in the liver. Consequently, it is not known if isoform specificity for TCE is the same in other tissues. Additionally, P450 isoform specificity in different animal species has not been thoroughly investigated. Differences among animal species in isoform content and specificity may, and likely does, play a role in the observed differences in metabolism and toxicity.

Lipscomb et al. (*11*) examined the oxidative metabolism of TCE in mouse, rat, and human liver microsomes and showed that TCE alters the metabolism of several chemicals that are characteristic substrates of CYP2E1 in all three species (*N*-dimethylnitrosamine-*N*-demethylase and *p*-nitrophenol hydroxylase), of CYP3A (benzoxyresorufin *O*-deethylase) in mice and rats, of CYP1A1/2 (ethoxyresorufin *O*-deethylase and phenacetin *O*-deethylase) in all three species, but had no effect on CYP2A (coumarin hydroxylase) activity. The effect of TCE was inhibitory for CYP2E1 and CYP3A and stimulatory for CYP1A1/2. These data confirmed earlier studies by Nakajima et al. (*40*) that CYP2E1 is the major hepatic isoform of P450 involved in TCE oxidation.

The broad range of halogenated hydrocarbons and other small organic molecules that undergo oxidation by CYP2E1 and the existence of several drugs and physiological or pathological conditions that may lead to induction of CYP2E1 indicate that certain conditions or prior or concurrent exposure to other chemicals, in particular ethanol, are important factors that must be taken into account in a risk assessment, since these may markedly alter the capacity for TCE metabolism by this pathway.

After formation of the TCE-oxygen-P450 (TCE-O-P450) or epoxide intermediate, CH (in equilibrium with chloral) is the major metabolite produced. In the liver, only small amounts of CH can be recovered as it is rapidly converted to other compounds. Hence, CH is not likely to be a major consideration for hepatotoxicity or hepatocarcinogenicity. In the lungs of male CD-1 mice, however, TCE produces Clara cell injury (*43,44*), and this has been attributed to the accumulation of CH, which occurs because the subsequent steps in the metabolism of CH are much slower than the conversion of TCE to CH (*45*). Besides having a slow rate of subsequent metabolism of CH, the rate of formation of CH in mouse lung is markedly higher than that in either rat or human lung (*44*). CH may be mutagenic, causing DNA damage, and is clastrogenic, producing aneuploidy. Although CH has been shown to be genotoxic (*45*), lung tumors resulting from CH are primarily benign, which is more consistent with a nongenotoxic, cell-proliferative mechanism. The cytotoxicity that can occur from the accumulation of CH, with subsequent repair mechanisms, may enhance cell proliferation leading to tumor formation. It should be noted, however, that the cytotoxicity of CH requires high concentrations to be accumulated, suggesting that the mouse lung is a specialized case and that this mode of action is probably not very relevant to that of TCE in other tissues or to other species.

In addition to CH, oxalic acid (OX), *N*-(hydroxyacetyl)aminoethanol, and DCA (through formation of an acyl chloride intermediate) may be formed from the TCE-O-P450 or TCE-epoxide intermediate (Figure

1). All four metabolites have been recovered in the urine of both laboratory animals and humans exposed to TCE. Subsequent metabolism is more complicated, involving multiple steps and other oxidative and reductive enzymes besides P450. With the exception of DCA, which is also formed by other mechanisms (see below), the other two metabolites are not likely to be of interest for understanding modes of action or risk assessment. CH is further metabolized to either TCOH or TCA, both of which can be further oxidized to DCA. A pharmacokinetic analysis of CH metabolism in $B6C3F_1$ mice provided evidence that was consistent with some formation of DCA directly from TCA (*46*). TCOH also undergoes glucuronidation, and TCOG has been recovered in the urine of animals and humans exposed to TCE. TCOG may also undergo enterohepatic recirculation and regenerate TCOH (see below).

CH reduction to TCOH has been reported to be inhibited by ethanol, and it was suggested that this reaction is, therefore, catalyzed by alcohol dehydrogenase (*47,48*). A recent study in mouse liver microsomes (*49*), however, found that pretreatment of mice with pyrazole, which induces CYP2E1, enhanced lipid peroxidation due to CH, whereas addition of a general P450 inhibitor reduced CH-induced lipid peroxidation. This suggested that metabolism of CH to TCOH and TCA is catalyzed primarily by CYP2E1. Furthermore, a human lymphoblastoid cell line expressing CYP2E1 metabolized CH to mutagenic metabolites, proposed to be derived from TCA and TCOH, whereas the parent cell line, which lacks CYP2E1, was inactive in CH metabolism (*50*). The proposed pathway of formation of the mutagenic metabolites in the transfected human lymphoblastoid cell line appeared to be similar to that in mouse liver microsomes. Since ethanol is metabolized in liver by both alcohol dehydrogenase and CYP2E1 and Larson and Bull (*47*) showed a dependence of the reaction on NAD^+, it is likely that both enzymes can be involved. The precise role of each enzyme in the reduction of CH to TCOH, however, remains to be determined.

Schultz and Weiner (*50*) found that the formation of TCOH from CH is stimulated *in vitro* by inclusion of ethanol in the reaction mixture. This, coupled with the *in vivo* data of Sellers et al. (*51*), supports the role of alcohol dehydrogenase in the formation of TCOH. The redox shuttling of cofactor-enzyme complex in the sequential reduction of CH and the oxidation of ethanol is enabled by the rate-limiting release of cofactor. The apparent contradiction with studies that have shown inhibition of alcohol dehydrogenase by CH may be explained by the substrate concentrations used. Data from Lipscomb et al. (*52*) imply that more than one enzyme is involved in TCOH formation in mouse liver. The increase in reaction rate is not observed at substrate concentrations above 0.5 mM (concentrations not likely to be observed *in vivo*). Analysis of kinetics data led Lipscomb et al. (*52*) to conclude that at higher substrate concentrations, a second, lower affinity enzyme becomes largely responsible for CH reduction. Similar kinetics, however, could not be demonstrated in rat or human liver cytosol.

Formation of trichloroacetate and dichloroacetate. TCA is produced by oxidation of either CH or TCOH. Oxidation of CH is believed to be catalyzed by an aldehyde oxidase, whereas oxidation of TCOH is catalyzed by P450, with CYP2E1 likely being the predominant isoform involved (*49*). As mentioned above, metabolism of CH to TCOH or TCA is slow in mouse lung, leading to accumulation of CH within the Clara cells. Overall, however, the lung plays a quantitatively minor role in CH metabolism. The subsequent reactions of CH are rapid in liver, leading to production of TCOH and TCA. Kinetics and time course studies in mice, rats, and dogs of TCE metabolism to CH, TCA, and TCOH are consistent with TCA being derived from oxidation of both CH and TCOH (*28,53–55*).

Lipscomb et al. (*52*) reported marked differences in CH metabolism to TCOH and TCA in liver and blood of rats, mice, and humans. Determination of kinetic parameters at physiologically obtainable concentrations of CH (i.e., in the range of 50 μM) showed that CH is cleared from human blood through hepatic metabolism at approximately 60% of the rate as in rodents. Hence, these data suggest that higher amounts of CH will be present in human blood and tissues than in those of rodents after a given exposure to TCE.

There has been considerable controversy and uncertainty about the sources and amounts of DCA formation, particularly in humans. Bull and colleagues (*54,56,57*) reported detection of DCA in urine of both rats and mice treated with TCA and in blood of mice treated with TCE. However, problems were reported with analytical methodologies that led to artifactual overestimations of DCA formation (*58*). The AUC for DCA following TCE administration to mice exceeded that predicted from the formation of TCA from TCE. Although other pathways for DCA formation have been proposed and may occur, it appears that in the presence of strong acids, some of the TCA that is in whole blood can undergo nonenzymatic conversion to DCA, thus leading to overestimation of DCA formation. In a subsequent study, Bull and colleagues (*55*) reassessed formation of metabolites of TCE in blood from rats, mice, and dogs, and found measurable levels of DCA only in blood from mice. Similarly, it is unclear whether DCA is produced in humans under normal circumstances. Henderson et al. (*59*) identified DCA, in addition to TCA, TCOH, and TCOG, as a metabolite of CH in children, for whom CH is still used therapeutically as a sedative–hypnotic agent. Nonetheless, more DCA is formed in mice than in other species. It is difficult, therefore, to develop parameters for DCA formation that can be used in PBPK models for human health risk assessment. Since both DCA and TCA produce hepatomegaly and cytomegaly that may lead to hepatocarcinogenesis (*54,56*) and DCA is derived from both TCA and TCOH, assumptions need to be made until a more definitive verdict on the formation of DCA in humans is made. However, both DCA and TCA are unequivocally hepatocarcinogenic, irrespective of their mechanism or mode of action (*54*).

An errata was published based on the studies of Templin et al. (*57*) and Abbas et al. (*46*) concerning artifacts in the determination of DCA. The bottom line is that the probable DCA concentrations in biological fluids are lower than those reported because of difficulties in analysis.

Formation of other oxidative end products. An additional problem with detection of DCA in biological samples, particularly tissue from liver, is the subsequent metabolism of DCA to other species, such as OX, CAA, glycolic acid, and glyoxylic acid (GLX). DCA has a much shorter half-life than TCA in rats and mice (*56*), consistent with rapid metabolism or excretion. Lipscomb et al. (*60*) described metabolism of DCA in liver cytosol from male $B6C3F_1$ mice and Fischer 344 (F344) rats that was dependent on reduced pyridine nucleotides and GSH but was oxygen independent. Stacpoole and colleagues (*61*) showed that liver cytosol from both rats and humans catalyzes the GSH-dependent conversion of DCA to GLX. The reaction is NAD(P)H-independent and exhibits a K_m for GSH of only 75 μM. It is unclear whether a GSH *S*-transferase (GST) isozyme is involved in the reaction.

Liver microsomes and mitochondria exhibit insignificant activity of DCA degradation (*60*). Hence, although dehalogenation of DCA to CAA may occur by P450-mediated catalysis, the major pathway(s) for hepatic DCA degradation appears to be P450-independent. In fact, Anders and Tong (*62*) recently showed that a newly described isoform of GST, GSTζ, is involved in the GSH-dependent oxygenation of DCA to form GLX.

The significance of these metabolites of DCA in TCE-induced toxicity and carcinogenesis is unclear, but their role is likely to be quantitatively minor. Little or trace amounts

above background of OX, CAA, glycolate, and GLX are detected in *in vivo* exposures to TCE or in *in vitro* incubations with TCE. OX is poorly soluble in water, leading to precipitates. Hence, extensive formation of OX might be expected to lead to formation of stones in the urinary tract.

Tissue Distribution of Oxidative Metabolism of TCE

Relative rates of oxidative metabolism of TCE in key target organs are important in understanding how these tissue-dependent differences affect toxicity. Besides P450, which catalyzes the initial step of TCE metabolism, tissue-dependent differences in secondary enzymes that act on metabolites of TCE, such as alcohol dehydrogenase and UDP-glucuronosyltransferase, may be important in that differences in these activities relative to P450 may alter the distribution of metabolites so that one or more metabolites may accumulate, leading to a pattern of toxicity that does not occur in tissues that have a different distribution of these activities.

Quantitatively, the liver is the most important site of oxidative metabolism of TCE due to the first-pass effect. Regardless of the route of administration (i.e., dermal, inhalation, oral), most of the TCE is rapidly absorbed into the circulation and goes to the liver. Only in specialized circumstances does the liver not play a key role or at least some role in determining overall metabolism and toxicity.

A situation where differential activities of the enzymes of the oxidative pathway of TCE metabolism markedly affect the distribution of metabolites and the toxicity is that of CH accumulation in mouse lungs (*44,45*). Clara cells of mouse lungs have relatively high P450 activity but have low activities of alcohol dehydrogenase and UDP-glucuronosyltransferase. Hence, the enzymes that metabolize CH and TCOH are believed to be present in low amounts relative to P450, leading to an accumulation of CH in the cells. Since TCOH is recovered in significantly greater amounts and as a higher fraction of total TCE metabolites in mice than in other species, UDP-glucuronosyltransferase may be present at relatively low levels compared to the other enzymes involved in oxidative metabolism of TCE, not only in the mouse lung, but in other mouse tissues as well, including the liver.

Besides the liver, the kidneys may be directly exposed to TCE or some of its metabolites, since they receive 25% of the cardiac output. While the kidneys contain P450 activities, including CYP2E1 (at least in rodents), most of it is in the proximal tubules and the total activity in the tissue as a whole is markedly lower than that in the liver. Nonetheless, renal oxidative metabolism of TCE occurs, albeit at rates that are 3- to 10-fold lower than those in the liver (*63*), and may play some role in either nephrotoxicity/nephrocarcinogenicity or, via renal–hepatic circulation, in liver injury.

Interorgan metabolism, which includes enterohepatic and renal–hepatic circulations of both the parent compound and several of the major oxidative metabolites, is another major issue in the development of models of TCE pharmacokinetics. Interorgan metabolism can also enhance the further biotransformation of TCE metabolites and has implications for target organ toxicity. For example, TCOG that is formed in the liver is excreted into bile, but little fecal excretion is observed due to extensive enterohepatic circulation. Once TCOG returns to the liver, it may be hydrolyzed back to TCOH and be metabolized further to TCA or DCA. In fact, TCA is the major circulating metabolite of TCE, likely due to its high affinity for binding to plasma proteins. A biphasic pattern of TCA concentrations is found in blood in the mouse (Table 2), consistent with enterohepatic circulation of TCOH. Thus, enterohepatic circulation plays a major role in the disposition of TCOH and TCOG. For the oxidative pathway of TCE metabolism, the major role for renal–hepatic circulation is in the excretion of metabolites in the urine. The major metabolites of TCE that are recovered in urine include TCA and TCOH/TCOG.

Sex- and Species-Dependent Heterogeneity in Oxidative Metabolism of TCE

As described in the reviews on mode of action in the various target organs, marked differences in susceptibility to TCE-induced toxicity are seen in males and females of each species and between species of a given sex. Since toxicity is directly associated with specific metabolites, the likely explanation for these differences in susceptibility are sex- and/or species-dependent differences in either overall rates of metabolism or distribution of metabolites among specific pathways. An understanding of the factors that determine these susceptibilities is essential for being able to extrapolate animal data to humans. An additional point, however, is that these sex- and species-dependent differences are often dose dependent in that markedly different types of effects may be seen at high versus low doses.

Overall rates of TCE metabolism vary considerably between the various experimental species that are used in laboratory investigations (i.e., rats, mice, rabbits) and between these species and humans (*64*). In practical terms, more complete documentation and understanding of sex- and species-dependent differences in metabolism will enable refinements in risk assessment and definitions of acceptable exposure levels. To extrapolate metabolic data between species in the development of pharmacokinetic models, default allometric scaling procedures are often used. These involve scaling fluid flows (e.g., blood, bile, urine) by body weight to the 3/4 power and scaling rate constants by body weight to the 1/4 power. Additional uncertainty factors are applied when there is uncertainty regarding intraspecies sensitivities or when there are uncertainties in extrapolating from one species to another. Again, these factors are intended to account for many processes, not just metabolism or pharmacokinetics. Whether these default assumptions are representative of the actual physiological state is an open question. For example, the activity of various P450s in humans can vary by up to a factor of 10 among individuals (*35,64,65*), so that default assumptions can be significantly different than the actual situation in humans. However, the observed variations are often beyond allometric expectations, suggesting that more complex metabolic and other differences exist between species.

As described earlier, studies by Prout et al. (*7*) showed that blood levels of the TCE metabolites TCOH, CH, and TCA were severalfold higher in B6C3F$_1$ mice than in Osborne-Mendel rats after a single oral dose of TCE. Larson and Bull (*54*) similarly showed that the initial rates of TCE metabolism to TCA were much higher in mice than in rats, leading to higher TCA concentrations in blood. Nakajima et al. (*42*) also showed that rates of oxidative metabolism of TCE in liver microsomes of male B6C3F$_1$ mice were 2- to 3-fold higher, depending on dose, than those from male Wistar rats. Furthermore, overall content of P450 (nmol P450/mg microsomal protein) did not differ in the two species. Rather, the higher rate of TCE metabolism was due specifically to higher levels of CYP2E1 in mouse liver microsomes. In general, metabolic rates for most chemicals are significantly higher in mice than in rats or other larger animals, including humans.

A comparison of kinetic parameters for overall P450-catalyzed metabolism of TCE in liver microsomes from male B6C3F$_1$ mice, F344 rats, and humans is shown in Table 4. Several species-dependent differences are immediately apparent. First, kinetics were clearly biphasic in liver microsomes from rat and human but were monophasic in liver microsomes from mouse. Rates of TCE oxidative metabolism for the high-affinity processes were approximately 2- to 2.5-fold faster than those for the low-affinity processes in rats and humans. Finally, the ratio of V_{max} to K_m values, which is a measure of catalytic efficiency, shows that although rates are lower than in the other species, the activity in

humans exhibits similar efficiency to that in rats and mice.

This similarity between rats and humans regarding P450-dependent metabolism of TCE may extend to other aspects of the metabolic process. Both the rat and human 2E family contain only one gene and expression of CYP2E1 in both species is regulated both transcriptionally and posttranscriptionally (*65*). In contrast, the rabbit 2E subfamily comprises two genes. Although rabbit CYP2E1 appears to be very similar to human and rat CYP2E1 with respect to substrate specificity and regulation of expression, rabbit CYP2E2 is not coordinately controlled with CYP2E1 and developmental expression of the two forms differs. Thus, Wrighton and Stevens (*65*) and Lipscomb et al. (*66*) concluded that the rat is a better model than the rabbit for study of human CYP2E1 expression. The data summarized above, comparing P450-dependent metabolism of TCE in rats, mice, and humans, support this conclusion and indicate further that the rat is a better model than the mouse for study of oxidative metabolism of TCE in humans.

Although sex-dependent differences have been clearly observed in the susceptibility to TCE-induced toxicity and carcinogenicity, few studies of sex dependence of TCE metabolism have been conducted. Nakajima et al. (*41*) studied sex-, age-, and pregnancy-induced effects on the expression and regulation of CYP2E1 and CYP2C11 with regard to TCE and toluene metabolism in Wistar rats. They observed no sex-dependent differences in TCE metabolism. The only differences in rates of TCE metabolism to CH that were observed were an approximately 3-fold decrease from 3 weeks of age (puberty) to 18 weeks of age (maturity) in both sexes and a nearly 2-fold decrease in rates in females during pregnancy.

Variations among Humans

Lipscomb et al. (*64*) observed considerable variability in the P450-catalyzed oxidation of TCE in 23 samples of human liver microsomes. K_m values for TCE (28.3 ± 12.9 μM; mean ± SD, n = 23) varied over a more than a fourfold concentration range (range = 12.6–55.7 μM) and were not normally distributed. V_{max} values for CH formation (1,589 ± 840 pmol/min/mg; mean ± SD, n = 23) also showed considerable variability, with samples from individual human livers exhibiting a 7-fold range of values (range = 490–3,455 pmol/min/mg). In their analysis of the kinetics of TCE metabolism, individual samples seemed to cluster into three groups, having K_m values (μM TCE, mean ± SD) of 16.7 ± 2.5 (n = 10), 30.9 ± 3.3 (n = 9), and 51.1 ± 3.8 (n = 4). Within each group, there were no patterns with regard to the ethnic group or sex of the donor from whom the livers were isolated, and V_{max} values in each group exhibited the same degree of variability and span of values as the entire sample pool. The K_m value in females (21.9 ± 3.5 μM; n = 10) were significantly lower than that in males (33.1 ± 3.5 μM; n = 13).

Analysis of the activity of three specific P450 isoforms that are known to catalyze TCE metabolism in human liver microsome samples from the three groups revealed some patterns (Table 5). CYP1A2 activity was significantly lower in the low-K_m group than in the other two groups, and CYP2E1 activity was significantly higher in the high-K_m group than in the two other groups, but no differences were observed for CYP3A4 activity among the three groups.

Lipscomb et al. (*64*) also found that CYP2E1 was the primary isoform responsible for TCE metabolism, accounting for > 60% of total microsomal metabolism. These results indicate that the capacity of humans to metabolize TCE will vary considerably and that factors that alter P450 activity, in particular CYP2E1 activity, can alter TCE metabolism and hence, susceptibility to TCE-induced toxicity. Nakajima et al. (*41*) also observed significant variation in oxidative metabolism of TCE as a function of physiological state (see above).

Comparative *in Vitro* Evaluation of Cytochrome P450-Dependent Metabolism of TCE

This section illustrates an integrated *in vitro* approach to evaluation of TCE metabolism by the P450 pathway with the goal of elucidation of the kinetics of metabolism of TCE to CH, TCOH, TCA, and DCA in the rat, mouse, and human. These data are based on a series of studies conducted at the Armstrong Laboratory (Toxicology Division at Wright-Patterson AFB, Ohio) (*11,52,60,64,67,68*). Data indicate *a*) that human hepatic microsomes possess less activity toward TCE than either rat or mouse hepatic microsomes, *b*) that TCOH formation proceeds at higher rates than TCA formation at low CH concentrations in all three species, and *c*) that appreciable levels of TCOH and TCA are formed from CH in the blood of all three species *in vitro*. The formation of DCA has been questioned for years, and no mechanism for its formation has been fully validated. DCA has not been identified in liver preparations (i.e., microsomes, homogenates, tissue slices) from mice or humans exposed to TCE, CH, or TCOH *in vitro*. Cultured gut microflora from mouse cecum produce DCA from TCA in a dose- and time-dependent

Table 4. Apparent kinetic constants for total oxidative metabolite formation from TCE.[a]

Species	V_{max} (nmol/mg per min)	K_m (mM)	V_{max}/K_m	n
Mouse				
Male	8.60 ± 4.50	0.38 ± 0.41	42.0 ± 28.5	5
Female	26.1 ± 7.3	0.16 ± 0.03	163 ± 37	3
Rat				
Male				
(High affinity)	0.96 ± 0.65	0.072 ± 0.082	23.8 ± 20.6	5
(Low affinity)	2.48 ± 0.97	0.482 ± 0.104	5.3 ± 2.2	
Female				
(High affinity)	2.91 ± 0.71	0.042 ± 0.021	80.0 ± 33.9	3
(Low affinity)	4.31 ± 0.31	0.111 ± 0.027	40.1 ± 7.1	
Human				
Male				
(High affinity)	0.52 ± 0.17	0.012 ± 0.003	48.0 ± 23.1	3
(Low affinity)	0.93 ± 0.17	0.093 ± 0.026	10.7 ± 3.9	
Female				
(High affinity)	0.33 ± 0.15	0.026 ± 0.017	15.3 ± 10.1	3
(Low affinity)	0.72 ± 0.60	0.160 ± 0.162	6.8 ± 5.6	

[a]Oxidative metabolism of TCE was measured by incubation of microsomes with 10 μM–2 mM TCE in the presence of 2 mM NADPH for 10 min at 37°C and pH 7.4. The following metabolites (assay limits of detection in parentheses) were measured after derivatization with pentafluorobenzyl bromide and gas chromatography with electron capture detection: TCA (1 ppm), DCA (0.025 ppm), CAA (0.025 ppm), OX (10 ppm). TCOH (0.001 ppm) was detected without any derivatization by gas chromatography with electron capture detection. CH (0.75 ppm) and GLX (0.1 ppm) were detected by HPLC after derivatization with 2,4-dinitrophenyl hydrazine. Data are means ± SD of measurements from the indicated number of experiments and were reported in Elfarra et al. (*70*).

Table 5. Evaluation of form-selective cytochrome P450 metabolism in human liver microsomes expressing different K_m values for TCE metabolism.[a]

Group	CYP form		
	CYP1A2	CYP2E1	CYP3A4
Low-K_m	241 ± 186	520 ± 295	2.65 ± 2.66[b]
Mid-K_m	545 ± 200	820 ± 372	2.92 ± 2.78[b]
High-K_m	806 ± 442	1,317 ± 592	1.78 ± 1.08[b]

[a]Activities of CYP1A2, CYP2E1, and CYP3A4 were measured with phenacetin, chlorzoxazone, and testosterone as substrates, respectively. Data are means ± SD of values from 10, 9, and 4 samples for the low-, mid-, and high-K_m group, respectively. Data within each isozyme assay with the same letter are not significantly different from one another ($p < 0.05$) by the Kruskal-Wallis one-way ANOVA.

manner. The transport of TCA from liver into blood or bile may influence net DCA formation; TCA in blood may be cleared into the urine, whereas TCA in bile enters the small intestine and may drive TCA production in the gut. However, in mice treated with antibiotics to eliminate gut microbes, plasma DCA concentrations following TCE treatment were only minimally affected, suggesting that non-gut mechanisms of DCA formation also exist. In summary, these *in vitro* studies indicate a lower rate of TCE metabolism and hence, a lower rate of TCA, TCOH, and DCA formation in the human as compared with the mouse and rat.

Chloral Hydrate Formation

Concentrations of TCE reported here, including K_m values, represent the concentration of TCE in the liquid phase of the incubation system. Gas chromatographic quantitation of CH and TCOH in the incubation mixture was accomplished by analysis of the ethyl acetate extract using modifications of the method of Maiorino et al. (*69*). Neither TCA nor DCA was detected (detection limit = 1.5 nmol/mL) under these conditions. Because CH is further metabolized to TCOH, CH and TCOH that were quantitated in microsomal incubations dosed with TCE were combined to give an estimate of TCE metabolism.

Significant differences between the three species were found in the Michaelis-Menten kinetic parameters evaluated for CH formation from TCE. Overall kinetic parameters for TCE metabolism in rat, mouse, and pooled human liver microsomes (Table 6) demonstrate a lower rate in the human than either the rat (1:3.3) or the mouse (1:3.8). Evaluation of these kinetic data over a wide range of TCE concentrations by construction of Eadie-Hofstee plots allowed for separation of data from rat liver microsomes into three kinetically distinct components, consistent with Nakajima et al. (*39*). The three components had K_m values (μM TCE) of 17, 114, and 909 μM and V_{max} values (pmol/min/mg) of 818, 1,275, and 2,797. A similar analysis of data from mouse liver microsomes revealed homogeneity, with only one kinetically distinct component. These results agree with those described above from Elfarra et al. (*70*).

Table 6. Overall kinetics of TCE metabolism to CH and TCOH.[a]

Species	K_m (μM TCE)	V_{max} (pmol/min/mg)
Rat	55	4,826
Mouse	35	5,425
Human	25	1,440

[a]Metabolism of TCE to CH and TCOH was measured in rat, mouse, and human liver microsomes by gas chromatography. Microsomes were pooled from 5 rodent and 7 human liver samples and were incubated with from 7.5 to 1,000 μM TCE for either 10 (rodent) or 30 (human) min.

As described above, evaluation of the data from individual human liver samples revealed considerable variation, with K_m values ranging from 16 to 56 μM and V_{max} values ranging from 490 to 3,455 pmol/min/mg, although there was no correlation between K_m and V_{max} values among individuals.

TCE was an effective inhibitor of CYP2E1, as measured by *p*-nitrophenol hydroxylase activity (data not shown). Three individual samples of human liver microsomes, representing individuals from the low-mid-, and high-K_m groups (see above), exhibited concentration-dependent inhibition of CYP2E1 activity. The degree of inhibition appeared to parallel the K_m of the microsomes for TCE metabolism, suggesting that CYP2E1 makes a larger contribution to TCE metabolism in the high-K_m sample than in either of the other two samples. Kinetic analysis of the inhibition of *p*-nitrophenol hydroxylase activity by TCE in mouse liver microsomes showed the inhibition to be competitive (data not shown), as would be expected if CYP2E1 metabolizes TCE.

To determine the extent to which CYP2E1 metabolized TCE in humans, experiments were designed using equivalent content of human CYP2E1, whether derived from human CYP2E1 gene transfected and expressed in a lymphoblastoid cell line or authentic human hepatic microsomes. The results (Figure 2) demonstrate that human CYP2E1 expressed in a lymphoblastoid cell line metabolizes approximately 75% as much TCE as an equivalent amount of authentic human liver microsomes. These data indicate that CYP2E1 is the major enzyme responsible for the microsomal oxidation of low concentrations of TCE in the human. To determine whether CYP2E1 was the predominant P450 form responsible for TCE metabolism in a sample of 27 human hepatic microsomes, the activity of a known substrate for CYP2E1, chlorzoxazone (CZX) (*71,72*), was compared with TCE metabolic activity (data not shown). Results indicate that TCE metabolism is significantly correlated (r^2 = 0.51, $p < 0.05$) with CYP2E1 activity in humans (*11*). These data provide further support for the involvement of CYP2E1 in TCE metabolism in the human.

The high degree of conservation of CYP2E1 across mammalian species and the high degree to which it is expressed in rodent liver, compared to human liver, make the determination of inherent CYP2E1 activity and the assessment of factors that modify CYP2E1 expression in the human important considerations in population risk assessments. To determine the variability of CYP2E1 and gain an indication of the potential variability of TCE metabolism in the human, microsomal metabolism of CZX and the degree of expression of total P450 content was examined in 54 human hepatic microsome samples (Figure 3). Data indicate that there is an approximate 5-fold variability in the expression of CYP2E1-dependent CZX metabolism in this population. Because of the degree of correlation of TCE metabolism with CYP2E1-dependent activity, it may be reasonably predicted that this degree of variability in TCE metabolism will be seen in the human population. Such variation and factors that induce the activity of CYP2E1 may define segments of the population that may be at a higher risk than would be otherwise anticipated (*73*).

The data also indicate that other enzymes may metabolize TCE in the human. Because a high fraction of P450 is accounted for by

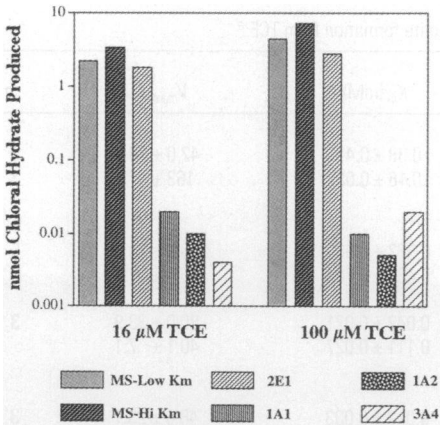

Figure 2. Metabolism of TCE by human liver microsomes and genetically-expressed P450 forms. Assays contained 1.0 mg liver microsomal protein/mL [which has been shown to contain 22 pmol of CYP2E1/mg protein (*73*)] or 22 pmol/mL of CYP2E1, 42 pmol/mL of CYP1A, or 96 pmol/mL of CYP3A4 expressed in microsomes from genetically engineered lymphoblastoid cells. Samples were incubated with 16 or 100 μM TCE and CH formation was measured after 30 min by gas chromatography.

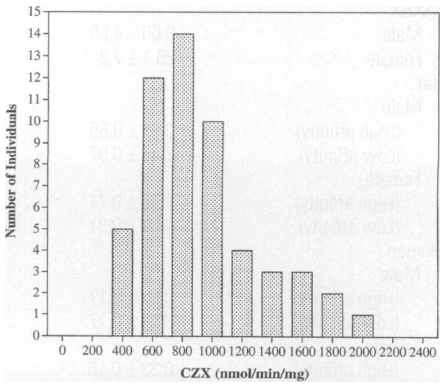

Figure 3. Distribution of CZX metabolism in a sample population of human liver microsomes. Histogram depicting the frequency distribution of metabolism of CZX, a marker substrate for CYP2E1, in individual human liver microsome samples. The results reveal a population with a normal distribution.

CYP3A4 and CYP1A2 (*72*), the effect on TCE metabolism of known substrates for these forms was evaluated. α-Napthoflavone (a CYP1A substrate) and ketoconazole (a CYP3A substrate) did not inhibit TCE metabolism when assessed at TCE concentrations near the K_m value (*64*) but reduced V_{max} values by 30 and 18%, respectively, when evaluated at TCE concentrations 4-fold above the K_m value. These data indicate that CYP1A2 and CYP3A4 also metabolize TCE in the human but that their contribution to overall TCE metabolism is low compared to that of CYP2E1.

Trichloroethanol and Trichloroacetic Acid Formation

TCOH is derived from CH. Species-dependent differences in the metabolism of CH were evaluated in a clarified liver homogenate (*52*). This preparation was used because various enzymatic activities capable of metabolizing CH are distributed in several subcellular compartments (*74*). NADH is the best nicotinamide cofactor for the stimulation of TCOH production *in vitro* in all three species. However, in human liver, NADPH also significantly stimulated TCOH production. For each of the cofactors tested, the addition of cofactor resulted in more TCOH production than in controls with no cofactor. The final evaluation of CH metabolism in the liver involved the determination of cofactor kinetics in the formation of TCOH. Data revealed that K_m* values (the concentration of cofactor that produced half-maximal metabolic rates) for these reactions in rodent liver approximated the levels of pyridine nucleotide cofactors reported for rodent liver (*75*). K_m* values (mM NADH) for TCOH formation were 0.91 and 0.36 mM for the rat and mouse, respectively.

An evaluation of clearance (V_{max}/K_m) of CH to TCA and TCOH was done to compare the net conversion of CH to these metabolites. The results in Table 7 indicate that clearance of CH to TCOH is much higher (10- to 200-fold) than clearance of CH to TCA in these three species. Clearance of CH to TCOH by the mouse high-affinity enzyme was highest, but this enzyme becomes inhibited at CH concentrations above 0.5 mM. Clearance of CH to TCOH in the human was approximately half that observed in rats and approximately twice that observed with the mouse low-affinity enzyme. Clearance of CH to TCA in the mouse and human were similar, whereas it was approximately 10-fold lower in the rat. These data indicate that TCOH formation will predominate over TCA formation in the liver of these three species. The kinetic evaluation of TCOH production also revealed that the mouse may have two separate enzymes responsible for formation of TCOH from CH in liver, whereas the rat and human apparently possess a single enzyme. The high-affinity form in the mouse is inhibited at CH concentrations above 0.5 mM (the nature of the inhibition is unknown), and the low-affinity form becomes saturated at concentrations of CH above 1.0 mM. This bifunctional metabolism is also seen in mouse hepatic cytosol (*76*). These results indicate that at least one mouse cytosolic enzyme responsible for TCOH formation becomes inhibited at high CH concentrations.

Table 7. Kinetics of TCOH and TCA formation from CH.[a]

	TCOH			TCA		
	K_m	V_{max}	V_{max}/K_m	K_m	V_{max}	V_{max}/K_m
Rat	0.52	24.3	46.7	16.4	4.0	0.24
Mouse				3.5	10.6	3.03
High affinity	0.12	6.3	52.5			
Low affinity	0.51	6.1	12.0			
Human	1.34	34.7	25.9	23.9	65.2	2.73

[a]Homogenate from the liver of 4 individuals from each species was centrifuged at 700×*g* and the supernatants obtained were pooled. K_m is presented as mM CH in solution that contained 0.9 mM NADH and 0.9 mM NAD^+ for experiments for TCOH and TCA formation, respectively. V_{max} is reported as nmol/min/mg 700×*g* supernatant protein. The mouse high-affinity enzyme responsible for TCOH formation was inhibited at CH concentrations > 0.57 mM.

TCA production from CH by mouse, rat and human liver supernatant was best stimulated by NAD^+. Of the reduced cofactors, only NADPH stimulated TCA production above that of control, and this occurred only in the mouse. These results (particularly the degree to which mouse liver TCA production is stimulated by both NAD^+ and $NADP^+$) indicate that there are species-related differences in hepatic TCA formation. The apparent kinetic constants for the formation of TCA from CH in the rat, mouse and human in the presence of NAD^+ indicate a much lower K_m value in the mouse, indicating that under equivalent CH concentrations, TCA formation will proceed at a more rapid rate in mouse liver (Table 7). It is doubtful whether CH will attain concentrations in human liver to drive metabolism near the theoretical maximal value. K_m values (CH) for TCA are much higher than those required for TCOH production, indicating that low concentrations of CH will favor the production of TCOH. K_m* values (mM NAD^+) for TCA production were 0.13 and 0.14 mM for the rat and mouse, respectively.

The kinetic parameters indicate that at low hepatic concentrations of CH (below 0.5 mM), TCOH will be the preferred hepatic metabolite. As shown in Table 8, the predicted ratio of TCOH:TCA is 10 to 20, depending on species. These predictions agree well with the observed urinary elimination of TCOH and TCA in mice and rats exposed to 200 mg TCE/kg (*53,54*) and with initial (0–1 hr) plasma levels of metabolites observed in CH-exposed humans, where the levels of TCOH were slightly higher than plasma levels of TCA (*51,77*). There is also evidence for the oxidation of TCOH to TCA (*77,78*). If TCOH is an obligate intermediate in the formation of TCA from CH, the accumulation of TCOH in blood and liver exposed to CH *in vitro* implies that the initial conversion of CH to TCOH is not rate limiting in the formation of TCA from CH.

Table 8. Predicted rates of hepatic metabolite formation at 50 μM chloral hydrate.[a]

	Metabolite	
Species	TCOH	TCA
Rat	2.13	0.012
Mouse	2.35	0.149
Human	1.25	0.136

[a]Metabolite (TCOH, TCA) formation is presented as nmol/min/mg 700 × *g* supernatant from liver homogenates of the indicated species. Metabolic rates were calculated from the Michaelis-Menten equation using the parameters obtained in Table 7.

Chloral Hydrate Metabolism by Blood

The conversion of CH to TCA and TCOH was examined in blood of the rat, mouse, and human to confirm and extend the findings of an earlier report (*51*), which demonstrated that significant amounts of TCOH and limited amounts of TCA were formed by blood *in vitro*. Results from experiments with lysed whole blood (no exogenous cofactor added) indicate that much more TCOH than TCA is produced (Table 9). Human blood produced less TCOH (on a milliliter-for-milliliter basis) than did either rat or mouse blood. However, TCA production in lysed human blood was significantly greater than TCA production by rat blood but only slightly higher than that by mouse blood. The further examination of lysed erythrocytes and plasma of the human indicate that erythrocytes were the sole site of blood TCA production (best stimulated by $NADP^+$). Plasma formed 4- to 5-fold as much TCOH from CH as did an equal quantity of packed erythrocytes, indicating that plasma is the primary site of TCOH production (best stimulated by NAD^+) by blood. These data underscore the need to evaluate the organ-specific, presystemic, extrahepatic formation and metabolism of CH derived from a TCE exposure and to fully describe CH metabolism in the blood compartment. Evaluation of the distribution of CH from portals of entry into

Table 9. Metabolism of CH to TCOH and TCA by lysed, whole blood.[a]

	Rat	Mouse	Human
TCOH	45.4 ± 4.9[b]	46.7 ± 1.0[b]	20.5 ± 0.7[c]
TCA	0.135 ± 0.020[d]	0.208 ± 0.030[e]	0.269 ± 0.030

[a]Results are presented as nmol product formed in a 400-µL lysate (containing 360 µL whole blood + 100 µL CH) over 30 min and are means ± SD of measurements from 3 experiments. Means with the same superscript letter are not significantly different from one another at $p < 0.05$.

blood and a kinetic examination of blood-catalyzed CH metabolism will further the success of species-dependent examination of CH metabolism *in vivo* and can be used to refine the PBPK models for both TCE and CH. Kinetic data would verify the importance of hepatic CH metabolism in the overall disposition of toxicologically relevant TCE metabolites.

Dichloroacetic Acid Formation from Trichloroacetic Acid

DCA is a TCE metabolite that is readily identified in rodents but is generally not identifiable in humans. DCA has not been detected under either aerobic or anaerobic incubations of hepatic fractions with TCE. While it has been impossible to demonstrate the hepatic formation of DCA from TCE *in vitro*, it has been demonstrated that the dechlorination of TCA to DCA is catalyzed by gut contents (ingested food and bacteria) of the rat and mouse. Microflora cultured from the cecum of the B6C3F$_1$ mouse dechlorinate TCA to DCA in a dose- and time-dependent manner (Figure 4) (*67*). To confirm these *in vitro* observations *in vivo*, B6C3F$_1$ mice were treated with antibiotics to virtually deplete the mouse gut of microflora. Antibiotic treatment resulted in dramatically increased gut TCA content and concurrently decreased gut DCA content compared with animals exposed to TCE without antibiotic. DCA present in circulating plasma was only slightly diminished in antibiotic-treated mice (*68*). Therefore, the source of DCA in plasma is still unknown.

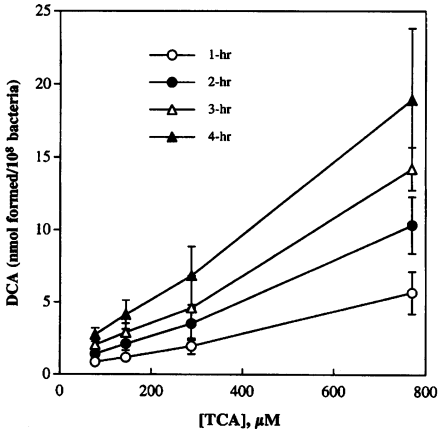

Figure 4. Time and concentration dependence of DCA formation by anaerobic mouse gut microflora cultures. Cultures of bacteria from mouse gut were incubated (10^8 cells/mL) with the indicated concentrations of TCA for up to 4 hr.

Dichloroacetic Acid Metabolism

DCA degradation occurs primarily in rat hepatic cytosol (*60*). Recent studies have revealed similarities between kinetic constants for hepatic cytosolic DCA degradation in the mouse and rat *in vitro* and marked differences between the kinetic constants in the human. These studies reveal K_m values of 350, 280, and 71 µM and V_{max} values of 13.1, 11.6, and 0.37 nmol/min/mg protein for the mouse, rat and human, respectively (*60*). Evaluation of clearance values (V_{max}/K_m) indicates that human liver cytosol degrades DCA less efficiently than either rat or mouse liver cytosol.

Species-Dependent Differences in P450-Dependent Metabolism of TCE: Interpretation of Findings for Human Health Risk Assessment

Several steps of the TCE metabolic pathway were evaluated *in vitro* and striking species-dependent differences were demonstrated. Kinetic parameters for several of the steps in the oxidative pathway of TCE metabolism are summarized in Table 10. All available *in vitro* data indicate that the human is less capable to metabolize TCE and CH than the rodent. The rate of CH formation in the human is approximately 20% of that of the mouse. Furthermore, *in vitro* kinetic parameters for TCE metabolism were not normally distributed in a sample of 23 human hepatic microsome preparations; K_m values were divisible into three statistically distinct groups. CYP2E1 is the form identified as the major determinant of TCE metabolism in the human, and the form is well conserved across species but is expressed to a higher extent in rodents than humans. CYP2E1 exhibits a K_m value for TCE of approximately 20 µM. The differential expression of CYP2E1 across species may in part explain the higher TCE metabolism seen in rodents than in humans *in vitro*. The examination of several sets of *in vitro* data also indicates that CYP1A and CYP3A forms metabolize TCE at concentrations above the K_m value for CYP2E1. The K_m value for TCE metabolism in microsomes of female humans is significantly lower than that in males, but V_{max} values were not significantly different (*64*). Factors that alter the expression or activity of CYP2E1 in the human should be incorporated into estimates of TCE metabolism *in vivo*. TCOH and TCA formation by components of mouse, rat, and human blood was demonstrated and TCOH was identified as the major blood-derived CH metabolite. The metabolism of CH to TCOH and TCA is efficiently catalyzed by liver homogenates from all three species, and TCOH formation predominated over TCA formation under all conditions evaluated *in vitro*. K_m values for TCOH formation are approximately 20-fold lower than K_m values for TCA formation, which drives the formation of TCOH at higher rates than TCA formation at low CH concentrations. K_m values for cofactor involvement in hepatic CH metabolism were shown to approximate cofactor concentrations found *in vivo*. These data indicate that significant changes in either cofactor level or redox status of the liver may impact the extent of CH metabolism and/or the ratio of TCOH:TCA produced. Such an impact has been demonstrated in the isolated perfused rat liver (*79,80*).

Table 10. Comparison of metabolic parameters for the oxidative metabolism of TCE determined *in vitro*.

Metabolic step	Mouse	Rat	Human
TCE to CH[a]			
K_m (µM TCE)	35.4	55.5	24.6
V_{max} (nmol/min/mg microsomal protein)	5,425	4826	1440
CH to TCOH[b]			
K_m (mM CH)	0.12 (low affinity) 0.51 (high affinity)	0.52	1.34
V_{max} (nmol/min/mg supernatant protein)	6.3 (low affinity) 6.1 (high affinity)	24.3	34.7
V_{max}/K_m	52.5 (low affinity) 12.0 (high affinity)	46.7	25.9
CH to TCA[b]			
K_m (mM CH)	3.5	16.4	23.9
V_{max} (nmol/min/mg supernatant protein)	10.6	4.0	65.2
V_{max}/K_m	3.03	0.24	2.73
DCA degradation			
K_m (mM DCA)	0.350[c]	0.280[d]	0.071[c]
V_{max} (nmol/min/mg cytosolic protein)	13.1	11.6	0.37
V_{max}/K_m	37.4	41.4	5.2

[a]Data reported in Lipscomb et al. (*8*). [b]Data reported in Lipscomb et al. (*52*). [c]Data reported in Lipscomb et al. (*165*). [d]Data reported in Lipscomb et al. (*61*).

DCA formation was not demonstrated in any tissue fraction evaluated *in vitro*. It was shown that gut contents of mice and rats dechlorinate TCA to DCA. Additional studies in antibiotic-treated mice *in vivo* revealed only slight depressions of plasma DCA levels following oral administration of TCE, indicating an additional, nongut source of DCA production. Because of the absence of DCA in samples from humans exposed to TCE, the degradation of DCA *in vitro* was evaluated. Human hepatic cytosol was less effective at degrading DCA than cytosol of rats or mice. These findings may explain the lack of demonstration of DCA in human blood following TCE exposure. Based on the assumption of equal rates of DCA formation across species, these results indicate that clearance of DCA by liver in the human does not account for the lack of finding DCA. Because TCA is also formed by components of blood, because TCA is more efficiently bound to plasma constituent proteins in the mouse than in the human, because binding of TCA by plasma proteins influences the distribution of TCA from blood to liver, and because TCA is equally well (if not more efficiently) formed in the liver of the mouse than of the human, it may follow that the human liver is less exposed to TCA than the mouse liver. If hepatic TCA concentrations drive biliary elimination of TCA, and TCA accumulation in the gut drives DCA formation, then it may be reasoned that DCA formation in the human is likely to occur at a much lower rate than in the mouse. However, gut is not the sole source of DCA formation. DCA levels in plasma were diminished but not eradicated in the antibiotic-treated mouse. These and other data complicate the inclusion of DCA in human health risk assessments of CH and TCE. The usefulness of *in vitro* data in the evaluation of the toxicity of TCE and human health risk assessment should be carefully weighed. While the traditional strength of *in vitro* data lies in mechanistic evaluations and the conditions employed do not reflect the total *in vivo* system, the accurate extrapolation of these (and other) *in vitro* data will yield important results. Precedent has been set for the use of *in vitro* data in PBPK models (e.g., *81*). A careful extrapolation of *in vitro* kinetic data from rat and mouse liver, the evaluation of pulmonary metabolism of TCE to CH, blood-mediated metabolism of CH to TCA, and plasma-binding characteristics of TCA will greatly aid the construction and validation of these models, lending credibility to the similar model constructed for the human (*11*). Evaluation of model effectiveness can be accomplished by comparing kinetic predictions with currently available human data. This *in vitro* approach will contribute to a valid, science-based, and technologically complex human health risk assessment for TCE.

Glutathione-Dependent Metabolism of TCE

This section describes the GSH conjugation (mercapturic acid) pathway for TCE. In classic drug metabolism textbooks, GSH conjugation has typically been described as a detoxication route for reactive electrophiles. For the majority of chemicals that are conjugated with GSH, this is a correct functional characterization. It became readily apparent several years ago, however, that GSH conjugation plays a bioactivation role for several types of drugs, particularly halogenated alkanes and alkenes. Although conjugation with GSH is the initial step in the pathway, the critical step for formation of a cytotoxic and/or carcinogenic metabolite occurs after processing to the cysteine conjugate. A major issue in the study of the conjugation of TCE with GSH and the toxicological consequences of this pathway is how to accurately measure flux through the pathway so that its importance relative to the P450 pathway can be assessed.

Description of GSH-Dependent Pathways of TCE Metabolism

GSH conjugation of TCE: formation of S-(1,2-dichlorovinyl)glutathione (DCVG). As shown in Figure 1, the other possible fate of TCE besides oxidative metabolism is conjugation with GSH, which is catalyzed by the GSTs. GSTs, like P450s, comprise a family of isoforms. With the exception of the microsomal GST isoform, all other isoforms are cytosolic. The primacy of the liver as the site of GSH conjugation is highlighted by the observation that GST protein can comprise as much as 5% of the total cytosolic protein in rat or human liver. However, GSTs are present in most tissues, including the kidneys, so that this initial step in the pathway does not necessarily have to occur in the liver but can also occur in the target organ.

The cysteine conjugate of TCE, *S*-(1,2-dichlorovinyl)-L-cysteine (DCVC), was discovered in a biological system nearly 40 years ago (*82,83*) when it was observed in soybean meal that had been extracted with TCE. DCVC was identified as the etiologic agent that caused nephrotoxicity and aplastic anemia in cows and only nephrotoxicity in several other mammalian species. For many years, DCVC was seen as a model compound that arose purely chemically rather than biochemically. An *in vivo* role for GSH conjugation in the metabolism of TCE was not appreciated until Dekant et al. (*84*) showed that the mercapturate of TCE, *N*-acetyl-*S*-(1,2-dichlorovinyl)-L-cysteine (NAcDCVC), was recovered in the urine of rats that had been exposed to TCE and Anders and colleagues (*85,86*) synthesized DCVG and demonstrated that it was nephrotoxic to rats and that it was metabolized to DCVC before exerting its toxicity. This suggested that a portion of TCE underwent GSH conjugation *in vivo* with subsequent processing to the cysteine conjugate followed by *N*-acetylation and urinary excretion of the mercapturate. Dekant et al. (*87*) subsequently showed that TCE was metabolized in rats to DCVG both *in vivo* and in isolated liver microsomes: After administration of TCE in corn oil by oral gavage, DCVG was recovered in the bile and NAcDCVC was recovered in the urine; DCVG formation was confirmed in rat liver microsomes incubated with TCE and GSH.

In a human TCE exposure study (*88*), healthy human volunteers (11 males, 10 females) were exposed for 4 hr by inhalation to either 100 ppm TCE (8 males, 8 females) or 50 or 60 ppm TCE (3 males, 2 females), and blood and urine samples were obtained at various time points both before and after exposure for up to several days. With respect to the current discussion of GSH-dependent metabolism of TCE, the most significant finding of these studies was that DCVG was detected in blood within 30 min of the end of the 4-hr TCE exposure period and its presence persisted for up to 12 hr. Both dose- and sex-dependent differences in DCVG levels in blood were detected and are summarized in Table 11. DCVG formation was clearly higher in males at both the higher and lower doses of TCE, consistent with the greater susceptibility of males to renal tumors from TCE [see review on "Mode of Action for Kidney Tumorigenesis" in this monograph (*89*)]. These data, therefore, demonstrate the function of the GSH conjugation pathway in humans. As discussed below, this is only the initial step in the generation of nephrotoxic species and does not directly correlate with it because subsequent detoxication reactions, such as mercapturate formation, can still occur.

GSH conjugation of TCE occurs at rates that are generally severalfold slower than the P450-catalyzed oxidation reactions. As mentioned above and discussed below in the section on the relative roles of the oxidative and GSH conjugation pathways in TCE-induced toxicity and carcinogenesis, there are several unresolved issues related to the importance of GSH conjugation in risk assessment for TCE. Rates of GSH conjugation of TCE are discussed below in more detail in the sections on tissue distribution and sex and species dependence.

Metabolism of DCVG to DCVC. DCVG, like other GSH conjugates, is processed by γ-glutamyltransferase (GGT) to the cysteinylglycine conjugate *S*-(1,2-dichlorovinyl)-L-cysteinylglycine (DCVCG) and then by various membrane-bound

Table 11. Formation of DCVG in blood from human volunteers exposed to TCE.[a]

	Maximal DCVG recovered (time after exposure)	
	Males	Females
50/60 ppm TCE		
nmol DCVG/mL blood	16.2 ± 8.1 (0.5 hr)	2.13 (1 hr)
pmol DCVG/mg protein	102 ± 81 (3 hr)	16.5 (1 hr)
100 ppm TCE		
nmol DCVG/mL blood	46.1 ± 14.2 (2 hr)	13.4 ± 6.6 (4 hr)
pmol DCVG/mg protein	517 ± 250 (3 hr)	138 ± 70 (4 hr)

[a]Healthy human volunteers (11 males, 10 females) were exposed by inhalation for 4 hr to either 50/60 ppm TCE (3 males, 2 females) or 100 ppm TCE (8 males, 8 females), and blood was collected at various times both before and after the exposure period. For analysis of DCVG, blood was deproteinated with acid and acid-soluble extracts were derivatized with iodoacetate and 1-fluoro-2,4-dinitrobenzene for analysis of *N*-dinitrophenyl–DCVG by ion-exchange HPLC using an amine column, a methanol–acetate solvent system with gradient elution, and detection at 365 nm. Maximal concentrations of DCVG recovered in whole blood, with the time after exposure indicated in parentheses, are shown below. Data were reported in (*88*). Results are the means ± SE of 3 sets of samples for males at 50/60 ppm TCE, means ± SE for 8 sets of samples for males or females at 100 ppm TCE, and the average of 2 sets of samples for females at 50/60 ppm TCE.

dipeptidases to DCVC (*90*). As will be discussed below, DCVC is the critical branch point in the metabolism of TCE by the GSH conjugation pathway. By this, it is meant that DCVC can be metabolized further by multiple enzymes to yield both detoxication products that are excreted and reactive species that have been associated with nephrotoxicity and are believed to be associated with nephrocarcinogenicity.

One strategy to validate the function of the GSH conjugation pathway in bioactivation and toxicity has been to use either cosubstrates that are specific for particular steps to potentiate activity or toxicity or to use specific inhibitors of enzymatic steps to inhibit pathway flux or toxicity. If the GSH conjugation pathway is responsible for bioactivation and toxicity, then cosubstrates should enhance toxicity and specific inhibitors should diminish toxicity. As summarized in Figure 5, this strategy has been applied to DCVG and its metabolites in both *in vivo* experiments (*85*) and *in vitro* studies with suspensions of isolated rat kidney cells (*91*). Hence, requirements for hydrolysis of DCVG by GGT was demonstrated with L-(α*S*,5*S*)-α-amino-3-chloro-4,5-dihydro-5-isoxazoleacetic acid (acivicin), a potent and irreversible inhibitor of GGT, and with a cosubstrate of the enzyme. Similarly, inhibitors of dipeptidase activity and of the β-lyase all prevented or greatly diminished cytotoxicity *in vitro* or nephrotoxicity *in vivo* of chemicals that occur before the inhibited step.

Metabolism of DCVC to NAcDCVC. In the classic view of the GSH conjugation pathway, cysteine conjugates undergo *N*-acetylation to yield mercapturates which, because of their polarity, are readily excreted in the urine. The *N*-acetylation reaction is catalyzed by a cysteine *S*-conjugate *N*-acetyltransferase found in the endoplasmic reticulum (*92*). This *N*-acetyltransferase is distinct from the cytosolic enzymes that are polymorphic in humans (e.g., isoniazid polymorphism). The mercapturate can also be deacetylated intracellularly, thus regenerating the cysteine conjugate. Hence, administration of NAcDCVC can also produce nephrotoxicity (*93,94*), and the relative rates of *N*-acetylation and deacetylation are important in determining the fraction of the mercapturate that can produce toxic metabolites.

Zhang and Stevens (*94*) compared the intracellular disposition and metabolic fate of DCVC and NAcDCVC in suspensions of rat renal proximal tubules. DCVC was rapidly transported into the tubules and was rapidly converted to NAcDCVC or was converted to reactive species that covalently bound to cellular proteins. Comparison of the amount of radiolabel covalently bound to cellular proteins with ^{35}S-DCVC and ^{35}S-NAcDCVC showed that a much higher proportion of radiolabel was bound from DCVC than from NAcDCVC. These data suggested that deacetylation of NAcDCVC is relatively slow. As described below, a significant portion of the DCVG that is formed in the liver is excreted into the bile and is converted there and in the intestines to DCVC. After enterohepatic circulation, some of this DCVC is converted to NAcDCVC in the liver and then excreted into the plasma and translocated to the kidneys. Hence, the relative amounts of DCVC and NAcDCVC that are released from the liver for translocation to the kidneys will modulate the amount of nephrotoxic and nephrocarcinogenic metabolites that are ultimately generated within the kidneys.

The NAcDCVC that is secreted into the tubular lumen of the kidneys or that arrives there by glomerular filtration and is not transported back into the renal epithelial cell for deacetylation is excreted into the urine. Indeed, NAcDCVC has been recovered in the urine of rats (*54,95,96*), mice (*97*), and humans (*17,96,97*) after exposure to TCE. This demonstrates that the GSH conjugation pathway for TCE occurs *in vivo*. Urinary NAcDCVC has been considered as a marker for flux of TCE through the GSH conjugation pathway, mostly for lack of a better alternative.

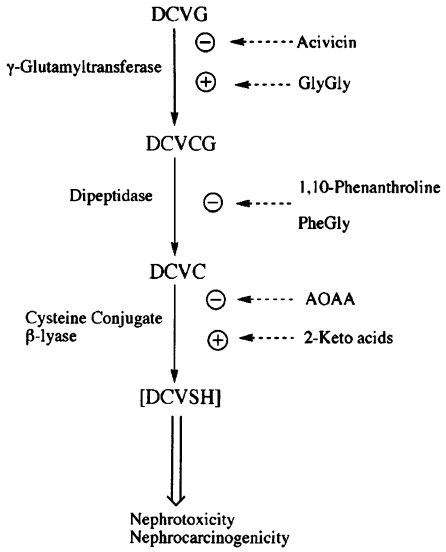

Figure 5. Validation of GSH conjugation and β-lyase pathway for bioactivation of DCVG. Abbreviations: GlyGly, glycylglycine; PheGly, phenylalanylglycine; AOAA, aminooxyacetic acid.

As described in the next and subsequent sections of this review, it is likely that urinary NAcDCVC represents only a small fraction of the total flux. Hence, although NAcDCVC may be reliably used to assess exposure to TCE, it will not be a very sensitive indicator owing to the small amounts recovered. More important for risk assessment, NAcDCVC has also been specifically considered as a marker of flux through the pathway that produces the nephrotoxic and nephrocarcinogenic metabolites of TCE. As described above, NAcDCVC is a detoxication product, whereas other metabolites of DCVC are the ones that are directly associated with renal injury. These considerations will be discussed further later in this review in relation to flux through the oxidative pathway of TCE metabolism and sex- and species-dependent differences in metabolism of TCE.

DCVC metabolism by β-lyase. Early studies with DCVC described its enzymatic breakdown by a C-S lyase in liver and kidney to pyruvate, ammonia, and an unidentified sulfur-containing fragment that formed covalent adducts with GSH and protein (*98*). Studies over the next three decades showed that the enzymatic activity, the β-lyase, is a family of pyridoxal phosphate (PLP)-containing enzymes that are found in several tissues besides the kidneys, including rat and human liver (*99–103*), intestinal microflora (*104,105*), and rat brain (*106,107*). However, many of these various β-lyase activities are catalyzed by distinct enzymes with varying substrate specificities or are not exposed to cysteine conjugates in the normal pathways of interorgan metabolism.

Although the DCVG that is formed in the liver and excreted into the bile can be degraded to DCVC and should then be available for

β-lyase–mediated catalysis by the intestinal microflora, these enzymes are not thought to play a significant role in DCVC metabolism and no intestinal toxicity is seen with administration of DCVC. As discussed below in the section on tissue distribution of β-lyase activity, the hepatic β-lyase activity is associated with kynureninase (*100*) and is distinct from the renal β-lyase activities (*108*), whereas the renal β-lyase activity is a catalytic property of glutamine transaminase K (*109–116*). Alberati-Giani et al. (*106*) reported that rat liver also expresses the mRNA for the renal glutamine transaminase K but that the levels of the mRNA in the liver are much lower than those in the kidneys. Due to the patterns of interorgan metabolism and the tissue specificity of enzymes that process GSH conjugates and related metabolites, hepatic kynureninase does not appear to play a role in DCVC metabolism and no liver pathology is observed after treatment of rats with DCVG or DCVC (*85,86,99*). Hence, it is the renal β-lyase activities that are critical for DCVC bioactivation.

The initial β-lyase activities that were purified from rat (*115*) and human (*113*) kidney cytosol were identified as catalytic activities of glutamine transaminase K with reported molecular weights of 85–100 kDa. Multiple β-lyase activities appear to be present in renal cortical mitochondria, a soluble form present in the matrix and identified with glutamine transaminase K (*116*) and a membrane-bound form that is distinct from glutamine transaminase K (*112*). Recent studies from Cooper and colleagues (*117,118*) have identified an additional, high-molecular-weight form of renal β-lyase with apparent molecular weight of 330 kDa. The high-molecular-weight form, like the low-molecular-weight form, is localized to the cytosol and mitochondrial matrix but is immunologically distinct from glutamine transaminase K and has no similarities to other known PLP-containing enzymes. Biochemical properties of the various renal β-lyase activities are summarized in Table 12. The apparent regulation of β-lyase activity by 2-keto acids (*110*), particularly in renal mitochondria, suggests that metabolic state may alter activity *in vivo*, thereby influencing toxicity. Keto acids stimulate renal β-lyase activity and potentiate DCVC-induced cytotoxicity in freshly isolated rat kidney cells because the β-lyase catalyzes both β-elimination and transamination reactions: During transamination, the PLP cofactor can become "trapped" in an inactive pyridoxamine phosphate (PMP) form in the absence of suitable keto acid acceptors; addition of exogenous keto acids converts to PLP, thereby restoring activity to the β-lyase (*110,115*).

As illustrated in Figures 1 and 5, DCVC is metabolized by the β-lyase to a reactive thiol, *S*-(1,2-dichlorovinyl)thiol (DCVSH). This thiol is chemically unstable and rearranges to reactive species that alkylate cellular nucleophiles (Figure 6). Trapping experiments were necessary to demonstrate formation of these metabolites due to their reactive and chemically unstable nature (*119*). Similar approaches have been used to trap and identify chemical structures of reactive intermediates from several other haloalkyl and haloalkenyl cysteine *S*-conjugates (*119–121*).

DCVC metabolites generated by the catalytic action of the β-lyase form covalent adducts with cellular nucleophiles, including proteins. Bull and colleagues (*122,123*) suggested that measurement of the acid-labile adducts could be used as an index of flux through the β-lyase pathway. While this would seem to make sense, as it is the quantity of the reactive species that is formed that can produce cellular injury and not, as discussed below, the quantity of stable endproducts that are excreted into the urine (e.g., mercapturates), the methodology is potentially complicated by artifacts due to chemical instability of the molecules being quantified. Additionally, Eyre et al. (*122,123*) found that apparent net activation of TCE by the β-lyase pathway and apparent acid-labile adduct formation were greater in mice than in rats, which does not correspond to the higher susceptibility of rats to renal toxicity and carcinogenesis, although adduct formation did correspond to increased cell replication rates. Hence, the relationship between adduct formation and effects on cellular function and homeostasis are very complex and require further study.

MacFarlane et al. (*124*) showed that pretreatment of rats with a single, subtoxic dose of the mercapturate of a nephrotoxic halogenated hydrocarbon produced a 1.5- to 3-fold increase in renal β-lyase activity and an increase in the cognate mRNA. These results suggest that prior or continuous exposures to low, subtoxic doses of certain cysteine or *N*-acetylcysteine conjugates may enhance the capability to generate reactive species by the β-lyase after subsequent exposures to toxic doses of these conjugates or their precursors. Although little is currently known about the genetic regulation of the β-lyase, these data suggest that differential expression of the β-lyase may need to be taken into account in a risk assessment for chemicals whose nephrotoxicity is mediated by this enzyme.

Direct demonstration of the function of the β-lyase *in vivo* in either experimental animals or humans has not been possible with DCVC because of the reactive nature of the metabolite. However, Iyer et al. (*125*) recently reported the identification of a metabolite of compound A (2-[fluoromethoxy]-1,1,3,3,3-pentafluoro-1-propene) that could only have arisen by β-lyase-dependent metabolism. Hence, this is the first study to directly show function of the β-lyase *in vivo* in humans.

DCVC metabolism by other enzymes. Although the β-lyase is considered to be the major bioactivation enzyme for DCVC, other bioactivation enzyme activities have been described, and some of these may have relevance to risk assessment. One of these other enzymes is the renal L-α-hydroxy (L-amino) acid oxidase (HAO), which can catalyze formation of the keto acid analogue of DCVC through an iminium ion intermediate, and this then decomposes to release DCVSH (*126,127*). This route of metabolism for DCVC has been estimated to account for as much as 35% of bioactivation in male F344 rats. HAO, however, is present only in rat kidney and is absent from human kidney. Thus, this pathway is irrelevant for human health risk assessment.

Table 12. Biochemical properties of mammalian renal cysteine conjugate β-lyase activities.

Property	Description
Subcellular localization	Cytosol and mitochondria (matrix and outer membrane)
Intrarenal localization	Predominantly S_3 segment of proximal tubule; also in S_1 and S_2
Molecular weight and subunit composition	Low-molecular-weight form: homodimer of 45–50 kDa each; aggregate M_r reported of 85–100 kDa; identical to glutamine transaminase K High-molecular-weight form: 330 kDa; at least two subunits of M_r 70 and 50 kDa; distinct from glutamine transaminase K
Cofactor	Pyridoxal phosphate
Substrate specificity	Both forms: good leaving group on beta carbon; haloalkyl or haloalkenyl cysteine *S*-conjugates are substrates. Low-molecular-weight form: nonhalogenated, alkyl-substituted conjugates are not substrates. High-molecular-weight form: leukotriene E_4 as a substrate.
Cosubstrate specificity	Both forms: 2-keto acids with relatively hydrophobic substituents on beta carbon (e.g., 2-keto-4-methiolbutyrate, phenylpyruvate). High-molecular-weight form: also activated by polar 2-keto acids (e.g., 2-ketoglutarate and pyruvate).
Reaction mechanism	Beta-elimination or transamination followed by reverse Michael elimination
Inhibitor	Aminooxyacetic acid

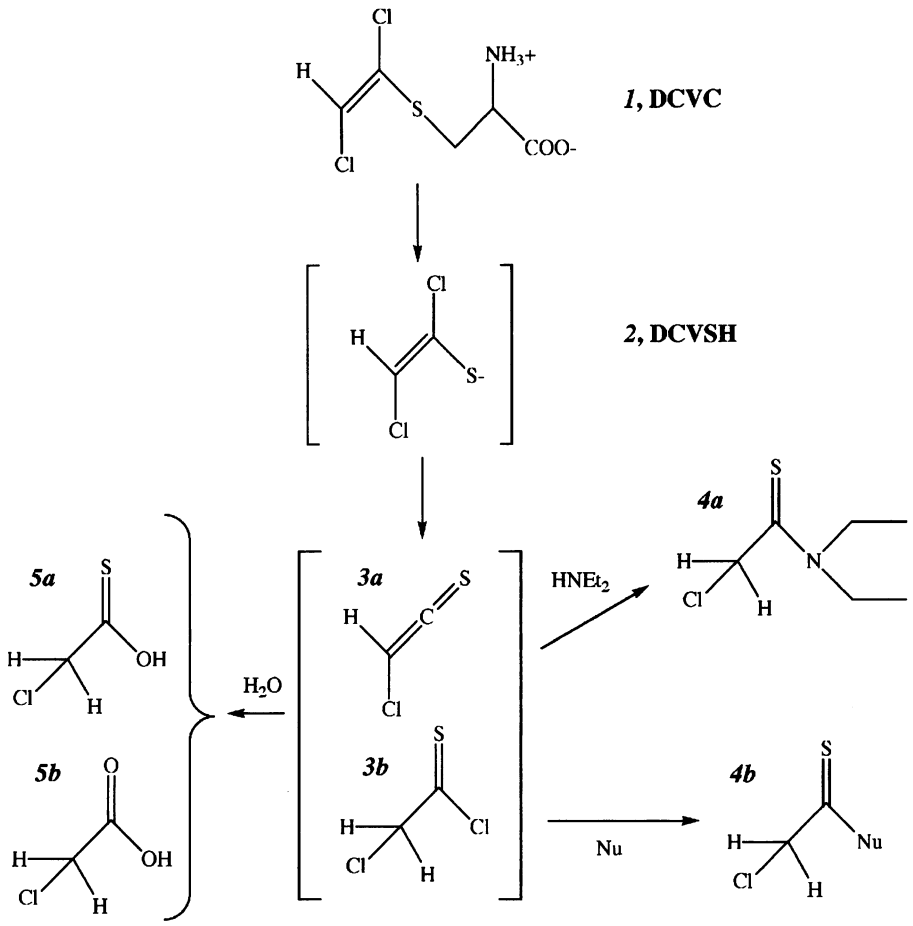

Figure 6. Scheme of formation of reactive metabolites from DCVC. Abbreviations: $HNEt_2$, diethylamine; Nu, cellular nucleophile. Metabolites: 1, DCVC; 2, DCVSH; 3a, chlorothioketene; 3b, chlorothionoacetyl chloride; 4a, *N,N*-diethylchlorothioacetamide; 4b, covalent adduct with cellular nucleophile; 5a, chlorothionacetic acid; 5b, CAA. Metabolite 4a is formed by trapping reactive metabolites 3a/3b with $HNEt_2$. Metabolites 5a and 5b are stable end products that are formed by hydrolysis. Modified from Dekant et al. (*119*).

Sulfoxides are known metabolites of cysteine conjugates that can be recovered in the urine as stable end products. Elfarra and colleagues (*128,129*) identified and subsequently purified an enzymatic activity from rat liver and kidney microsomes that metabolizes DCVC to its sulfoxide. This enzyme was subsequently shown to be a flavin-containing monooxygenase (FMO), initially thought to be related to FMO1A1 (*129*), but more recent data suggest that FMO3 is the isoform responsible for DCVC oxidation (*130*). Unlike other cysteine conjugate sulfoxides, DCVC sulfoxide is unstable and reacts with cellular nucleophiles, including GSH (*131*). The potential significance of this activity for overall TCE or DCVC bioactivation and for human health risk assessment is unclear, but DCVC sulfoxide was shown to be markedly more nephrotoxic to rats and more cytotoxic in freshly isolated rat renal cells than DCVC (*132*). This finding warrants further investigation.

Werner et al. (*133*) recently showed that sulfoxides can arise by a different pathway. In their studies, they found that NAcDCVC and the mercapturate of perchloroethylene (PER) were metabolized by rat liver microsomes to the corresponding sulfoxides by CYP3A and not by an FMO. These investigators also found that the *N*-acetylcysteine conjugate sulfoxides were markedly more cytotoxic in freshly isolated rat renal cortical cells than the corresponding mercapturates, similar to the situation with cysteine conjugate sulfoxides. This report adds an additional dimension to known bioactivation mechanisms of DCVC. Due to the efficient processing of mercapturates by the liver, which leads to their delivery to the kidneys, and the much lower activity of CYP3A in the kidneys as compared with the liver, this pathway is not likely to be quantitatively important overall or even in comparison to the β-lyase pathway.

An additional although minor fate of the reactive DCVSH generated by the β-lyase and other enzymes is methylation, which occurs by a thiomethyltransferase in the intestinal microflora (*134*). The thiomethyltransferase uses *S*-adenosylmethionine to transfer a methyl group to the thiol, forming the methylthio derivative, which is subsequently oxidized to the methylsulfinyl (CH_3SO–) and methylsulfonyl (CH_3SO_2–) analogs. The methylthio derivatives are nonpolar and are generally excreted into the feces. Quantitatively, this pathway is probably minor for TCE, accounting for no more than 0.05–0.1% of the total excreted metabolites of TCE.

Membrane transport of GSH-derived metabolites of TCE. Membrane transport processes play an important role in the tissue distribution of the various GSH conjugates and related metabolites [(*89*); also see discussion below on interorgan metabolism). There are three GSH-derived metabolites of TCE whose membrane transport is important for understanding tissue distribution: DCVG, DCVC, and NAcDCVC. For DCVG, both efflux from the hepatocyte and membrane transport processes in renal proximal tubular cells are toxicologically important. For both DCVC and NAcDCVC, uptake into renal proximal tubular cells is the relevant process.

As discussed above, there are two primary sources or sites of formation of DCVG—the liver and the kidneys. For DCVG that is generated by renal GSTs, further processing occurs by efflux of intracellular DCVG by transport across the brush-border membrane into the lumen, where it can then be metabolized by GGT and dipeptidases to generate DCVC. Efflux of GSH and GSH *S*-conjugates into the lumen by transport across the brush-border membrane is viewed as an essential step in the turnover of these compounds because the active site of GGT is extracellular (*135*). In fact, inhibition of GGT *in vivo* produces marked glutathionuria in mice (*135*). Presumably, a marked increase in urinary excretion of GSH conjugates would also occur under similar conditions. Although this transport step has not been specifically quantitated for DCVG, Inoue and Morino (*136*) determined the mechanism and kinetics of transport for GSH in renal brush-border membrane vesicles. GSH uptake was dependent on the membrane potential and exhibited a K_m for GSH of 0.21 mM and a V_{max} of 1.15 nmol/min per mg protein. It can be expected that brush-border membrane DCVG transport will likely exhibit similar kinetics.

For DCVG that is generated in the liver, there are two additional steps, efflux across the canalicular membrane into the bile or across the sinusoidal membrane into the plasma, and extraction by the kidneys. Hepatic GSH conjugates are transported primarily into bile by the canalicular multispecific organic anion transporter (cMOAT), which is an ATPase that mediates efflux of various GSH conjugates and organic anions (*137–140*). Again, transport of DCVG by this carrier has not been specifically studied. However, kinetics for transport of the model GSH conjugate

S-(2,4-dinitrophenyl)glutathione (DNPSG) have been characterized. K_m (μM DNPSG) and V_{max} (nmol translocated/min per mg protein) values of 71 and 0.34, respectively, were reported by Akerboom et al. (*137*), whereas Niinuma et al. (*140*) reported values of 18 and 1.15, respectively. Comparisons with other model GSH conjugates reveal some variability in rates of transport (up to a 5-fold range), suggesting that these values for DNPSG should only be used as a rough estimate for the transport of DCVG from the hepatocyte into the bile. Although data in normal human liver are not available, Olive and Board (*141*) characterized efflux of DNPSG from eight different cultured human liver cell lines, including Jurkat, HL-60, HepG2, and HeLa cells. A 10-fold range of transport rates was observed. These cells also exhibited a 6-fold range of intracellular GSH contents and a 5-fold range of GST activities. However, there was no correlation between transport activity and either GSH content or GST activity. Hence, although transport data from normal human liver is unavailable, these studies in cell lines suggest that considerable variations in transport capacity may exist.

Besides the luminal transport of DCVG, plasma DCVG that does not undergo glomerular filtration may gain access to the renal proximal tubular cell by transport across the basolateral plasma membrane (*142*). This transport occurs by the Na^+-coupled system described for GSH (*143,144*). Transport of both GSH and GSH *S*-conjugates is inhibited by probenecid and *p*-aminohippurate, suggesting that the organic anion carrier may be involved in the transport. Another study on renal plasma membrane GSH transport (*145*) indicates the additional involvement of plasma membrane dicarboxylate carriers. Rates of DCVG transport into membrane vesicles were extremely rapid (22 nmol/min/per mg protein with 5 mM DCVG) and transport was inhibited by GSH and γ-glutamyl amino acids, but not by DCVC (*142*). Once inside the renal proximal tubular cell, DCVG will be translocated to the brush-border membrane for efflux into the lumen and metabolism as described above.

Once DCVG is secreted into the bile, a significant portion of it will be metabolized by either biliary or intestinal GGT and dipeptidases to form DCVC. The transport processes relevant for DCVC include uptake into the hepatocytes (enterohepatic circulation) and uptake into the renal proximal tubular cell. Again, little data are available on rates of DCVC transport into the liver, with the exception of one *in vitro* study. Simmons et al. (*146*) characterized DCVC uptake by isolated canalicular membrane vesicles from rat liver. DCVC uptake was Na^+ independent and exhibited K_m and V_{max} values of 155 μM and 4.7 nmol/min per mg protein, respectively. This step thus appears to have a greater capacity than any of the steps for DCVG transport.

Renal extraction of plasma DCVC can occur by either glomerular filtration and uptake across the brush-border membrane or by uptake across the basolateral membrane. Transport across the brush-border membrane from rat kidney cortex was reported to be Na^+ dependent and exhibited K_m and V_{max} values of 225 μM and 3.1 nmol/min per mg protein, respectively (*147*). In contrast, Wright et al. (*148*) found that DCVC uptake in brush-border membrane vesicles from rabbit renal cortex was Na^+-independent and exhibited K_m and V_{max} values of 0.45 mM and 60 nmol/min per mg protein. Brush-border membrane transport of DCVC was unaffected by NAcDCVC or several other organic anions but appears to occur by the same carrier that transports neutral amino acids such as phenylalanine. In contrast to this, basolateral transport of DCVC occurs by both Na^+-dependent and Na^+-independent mechanisms and the Na^+-dependent process interacts with the transport of NAcDCVC and organic anions (*149,150*). Rates of DCVC uptake by isolated renal proximal tubular cells, which reflect primarily transport processes occurring at the basolateral membrane, were approximately 2-fold higher for DCVC than for DCVG (*142,150*). Thus, as with canalicular membrane transport, renal transport of DCVC appears to be significantly faster than that of DCVG.

After release from the hepatocyte, DCVG will undergo interorgan translocation and/or metabolism. In its translocation to the kidneys, a portion of it will first be returned to the liver before efflux into plasma (renal-hepatic circulation). Some of the DCVG will be metabolized extrahepatically to DCVC and some of this will be *N*-acetylated, either extrahepatically or in the liver to form NAcDCVC. Hence, the mercapturate is also a form to which the kidneys are exposed. Transport of NAcDCVC into renal proximal tubular cells occurs readily and presumably by the organic anion carrier (*93,94*). Kinetic parameters for transport at specific membrane sites are unavailable, but estimates appear to be similar to those for DCVC. Transport of NAcDCVC is not believed to be limiting for nephrotoxicity, as described above. Rather, the intracellular deacetylation reaction likely determines the extent of regeneration of DCVC and the degree of cytotoxicity.

Tissue Distribution and Sex- and Species-Dependent Heterogeneity of GSH-Dependent Metabolism of TCE

The selective tissue distribution of the various enzymes of the GSH-dependent metabolism of TCE plays a critical role in determining the target organ specificity of DCVC and the reactive species that are derived from its further metabolism. Hence, a precise knowledge of the relative activities of each of the major enzymes of the pathway is important, to help both in understanding how toxicity occurs and in assessing the relevance of the GSH conjugation pathway relative to the oxidative pathway in TCE-induced toxicity. The liver and kidneys are the major sites of GSH-dependent metabolism of TCE, although biliary and intestinal metabolism also play significant roles.

Although most cell types express some GST activity, the liver is by far the predominant site of GSH conjugation. Table 13 summarizes measurements of GST activity with 1-chloro-2,4-dinitrobenzene as substrate in cytosolic fractions from male and female F344 rat and $B6C3F_1$ mouse liver and kidney. With the exception of the female rat, specific activities (normalized to protein) are slightly to modestly lower in kidney cytosol than in those from liver cytosol. However, total activity in the liver will be much higher than in the kidneys due to the larger tissue size.

For chemicals such as TCE that undergo GSH conjugation and eventually are translocated to the kidneys for further metabolism, it has generally been assumed that most if not all of the GSH conjugation occurs in the liver. However, Lash et al. (*151*) showed that TCE is conjugated with GSH in freshly isolated kidney cells from male F344 rats, although at rates that are only 5 to 10% of those in isolated hepatocytes (Figure 7). Koob and Dekant (*152*) also demonstrated that hexafluoropropene, a nephrotoxic fluoroalkene, can undergo GSH conjugation in the kidney as well as in the liver. Thus, the entire GSH conjugation pathway can occur within the target tissue. Although the majority of the flux involves interorgan processes (see below), with the liver catalyzing the majority of the initial step in the pathway, this intraorgan process should be taken into account in refinements of PBPK models and risk assessments for TCE.

A summary of measurements of DCVG formation from TCE in liver and kidney cytosol and microsomes from male and female F344 rats and $B6C3F_1$ mice (*153,154*) is given in Table 14. The results show some dramatic sex- and species-dependent differences in GSH conjugation of TCE. Although overall GSH conjugation in male rats is clearly higher than that in female rats, no detectable DCVG formation was observed in male rat liver microsomes, whereas DCVG formation in female rat liver microsomes occurred at approximately twice the rate as in the cytosol. Rates of metabolism in mice in both kidney and liver fractions were also generally faster in males than in females and were markedly higher than corresponding rates in

rats. This last point brings up an interesting correlation with the covalent adduct formation reported by Bull and colleagues (*93,94*). As summarized above, 2-fold higher rates of covalent adduct formation from ^{35}S-labeled DCVC were found in mouse kidney compared to those in rat kidney. Hence, both higher rates of adduct formation and GSH conjugation of TCE occur in the mouse kidney, although the rat is the species in whom renal tumors are observed.

Kinetics of GSH conjugation of TCE in subcellular fractions from pooled human liver and kidney samples are summarized in Table 15. Although analysis could only detect a single, kinetically distinct process for DCVG formation in kidney fractions, GSH conjugation of TCE in both liver cytosol and microsomes were resolved into two kinetically distinct processes. Maximal rates of DCVG formation in human liver and kidney were only modestly lower than those in rat liver and kidney but were approximately 5-fold lower than those in the mouse. Hence, it appears that any limitation in the generation of reactive metabolites of TCE from this pathway does not exist at the initial step where DCVG formation occurs. Rates of GSH conjugation of TCE in human liver and kidney subcellular fractions reported here are up to an order of magnitude greater than those reported by Green et al. (*154*). In incubations with 1.9 mM TCE and 5 mM GSH, Green and colleagues found rates of DCVG formation of 2.5, 1.6, and 0.19 pmol/min per mg protein in liver cytosols of male mice, rats, and humans, respectively. In contrast, in incubations with 2 mM TCE and 5 mM GSH, Lash and colleagues (*151,153,155*) reported rates of DCVG formation of 408, 122, and 5,770 pmol/min per mg protein in liver cytosols of male mice, rats, and humans, respectively. Similarly, Green et al. (*154*) were unable to detect net, enzymatic formation of DCVG in incubations with rat kidney subcellular fractions. In contrast, Lash and colleagues (*151,153*) reported a rate of DCVG formation in incubations of male rat kidney cytosol with 2 mM TCE and 5 mM GSH of 7.5 pmol/min per mg protein and a rate of 0.7 nmol/min per mg protein in pooled human kidney cytosol (*154*).

The controversy between these results has not been resolved. Differences in analytical methods (radiolabeled substrate with high performance liquid chromatography (HPLC) separation versus derivatization and HPLC separation) may contribute to the discrepancies in measured rates. Beyond this, no other explanations are available to explain the discrepancies. Green and colleagues (*154*) also reported that formation of DCVG was linear with respect to incubation time for at least 60 min, whereas Lash et al. (*151,153*) showed the expected saturation kinetics and maximization versus incubation time of an enzyme-catalyzed process.

Measurements of GGT activity in liver and kidney subcellular fractions from male and female rats and mice and pooled human liver and kidney samples show clearly that at least in rodents, insignificant GGT activity is present in the liver (Table 16). Human liver exhibits relatively low activity of GGT (approximately 3% of that in the kidneys). Only modest sex-dependent differences were observed in GGT activity. Rats exhibited the highest activity of GGT, with humans exhibiting approximately 50% of that in rats and mice exhibiting only 20% of that in rats. Higher GGT activity provides more substrate for the β-lyase reaction, which would generate higher amounts of reactive species. Hence, these differences may contribute to species-dependent differences in overall flux of TCE through the GSH conjugation pathway.

Hinchman and Ballatori (*156*) compared renal and hepatic GGT activity in several mammalian species. Although the kidneys contain the highest levels of GGT activity in all species examined, including humans, specific activities (i.e., mU/mg protein) can vary up to 10-fold or more between species. Furthermore, although adult liver contains relatively low levels of GGT activity, specific activities can also vary up to 10-fold or more. Hence, while the ratio of GGT specific activity in kidney to that in liver was reported as 875 in rats and 413 in mice, it was only 100 in rabbits and 19 in pigs. Humans exhibit tissue distributions similar to rabbits. Use of rats to model

Table 13. Measurements of GST activity in liver and kidney cytosol from male and female F344 rats and B6C3F$_1$ mice.[a]

Sex	Species	Tissue	Activity (mU/mg protein)
Male	Mouse	Liver cytosol	0.78 ± 0.28
Male	Mouse	Kidney cytosol	0.70 ± 0.09
Female	Mouse	Liver cytosol	0.49 ± 0.03
Female	Mouse	Kidney cytosol	0.34 ± 0.04
Male	Rat	Liver cytosol	1.10 ± 0.44
Male	Rat	Kidney cytosol	0.55 ± 0.10
Female	Rat	Liver cytosol	0.28 ± 0.06
Female	Rat	Kidney cytosol	0.34 ± 0.08

[a]GST activity was measured spectrophotometrically with 1 mM 1-chloro-2,4-dinitrobenzene as substrate by determining formation of 2,4-dinitrophenylglutathione at 340 nm. Results are the means ± SE of measurements from 6 experiments for rats and 4 experiments for mice. Data reported in (*153*).

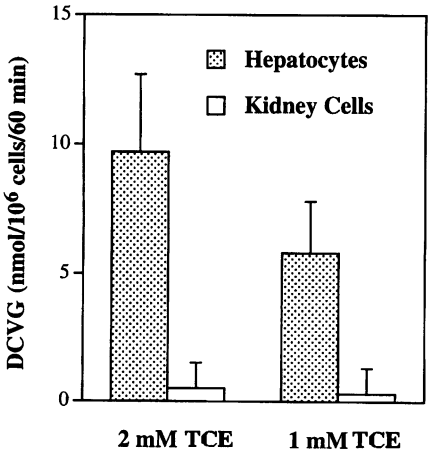

Figure 7. GSH conjugation of TCE in suspensions of freshly isolated hepatocytes and renal cortical cells from male F344 rats. Isolated hepatocytes (2×10^6 cells/mL) or renal cortical cells (8×10^6 cells/mL) were incubated with 1 or 2 mM TCE in the presence of 5 mM GSH at 30°C for 60 min. DCVG formation was measured by ion-exchange, reversed-phase high-performance liquid chromatography after derivatization with iodoacetate and 1-fluoro-2,4-dinitrobenzene, and was detected by absorbance at 365 nm. Results are the means ± SE of 3 experiments. See (*150*) for other details.

Table 14. Summary of metabolism of TCE by GSH conjugation in kidney and liver subcellular fractions from male and female F344 rats and B6C3F$_1$ mice.[a]

Subcellular fractions	DCVG formation (nmol/mg protein or 10^6 cells per 60 min) Male	Female
Rat kidney cells	0.48 ± 0.02	0.65 ± 0.15
Rat hepatocytes	9.70 ± 0.29	2.67 ± 0.69
Rat kidney cytosol	0.45 ± 0.22	0.32 ± 0.02
Rat kidney microsomes	ND	0.61 ± 0.06
Rat liver cytosol	7.30 ± 2.80	4.86 ± 0.14
Rat liver microsomes	10.3 ± 2.8	7.24 ± 0.24
Mouse kidney cytosol	5.60 ± 0.24	3.70 ± 0.48
Mouse kidney microsomes	5.47 ± 1.41	16.7 ± 4.7
Mouse liver cytosol	24.5 ± 2.4	21.7 ± 0.9
Mouse liver microsomes	40.0 ± 3.1	25.6 ± 0.8

ND, not detectable; limit of detection was 0.05 nmol/mg protein or 10^6 cells. [a]Results are means ± SE of measurements from 3 separate cell or tissue preparations and are for 2 mM TCE incubated with 5 mM GSH for 60 min. DCVG formation was measured after derivatization of acid extracts with iodoacetate and 1-fluoro-2,4-dinitrobenzene, separation by ion-exchange, gradient HPLC on an amine column using a methanol–acetate mobile phase and detection of *N*-dinitrophenyl DCVG at 365 nm. Data reported in (*151,153*).

Table 15. Kinetics of GSH conjugation of TCE in human kidney and liver subcellular fractions.[a]

Tissue/subcellular fraction	V_{max} (nmol DCVG/min/mg protein)	K_m (μM TCE)
Kidney		
Cytosol	0.81	26.3
Microsomes	6.29	167
Liver		
Cytosol: low affinity	8.77	333
Cytosol: high affinity	4.27	22.7
Microsomes: low affinity	3.10	250
Microsomes: high affinity	1.42	29.4

[a]Activity of GSH conjugation of TCE was measured in cytosol and microsomes from pooled human liver and kidney samples. Fractions (1 mg protein/mL) were incubated with 7.8 μM–1 mM TCE and 5 mM GSH at 37°C; DCVG formation was quantitated by HPLC analysis after derivatization. Kinetic parameters were calculated from Eadie-Hofstee plots and are derived from measurements from 3 separate incubations. Results were reported in (*155*).

interorgan GSH and GSH *S*-conjugate metabolism thus overestimates the role of these pathways in turnover. This is not to say, however, that the interorgan pathways do not play a significant role even in humans, since total renal activity is still severalfold higher than that of total hepatic activity.

A scheme summarizing the interorgan processes involved in GSH conjugation and subsequent metabolism of TCE is shown in Figure 8. Processes occurring in the liver, small intestine, kidneys, bile, and plasma are highlighted. Although most studies that were performed in the development of this model have used the rat, the interorgan metabolism model is valid in humans, although fluxes and distributions of metabolites in the various compartments (i.e., plasma, bile) will vary. TCE is shown as having two fates: being taken up by the liver where it is conjugated with GSH or being taken up by the kidney where it may also be conjugated with GSH. The two principal interorgan pathways are the enterohepatic and renal–hepatic circulations. The determining factors in these pathways are the following: *a*) high activity of GST in the liver; *b*) efficient transport systems in liver cells for efflux of GSH conjugates into bile or plasma; *c*) relatively high activity of GGT on renal brush-border membranes and relatively low activity of GGT in liver; and *d*) selective presence of a transport system for uptake of GSH conjugates on renal basolateral membranes and the absence of an uptake system in liver cell plasma membranes.

GSH conjugation of TCE was demonstrated in isolated human hepatocytes (Figure 9). Rates of DCVG formation, although lower than those in rat hepatocytes by approximately 2- to 3-fold, were not so low or difficult to detect that one would conclude that flux through the GSH conjugation pathway is too low to account for a measurable and possibly significant portion of total TCE metabolism. Of course, this is only the initial step in the pathway with subsequent branches leading to excretion of nontoxic products in addition to the branches that produce toxic metabolites. Hence, it is critical to quantitate formation of the metabolites that directly produce cellular injury.

As emphasized above, the key step in the bioactivation of TCE by the GSH conjugation pathway is the β-lyase step. Reports of β-lyase activity in the literature show a fair amount of variability, depending in part on the cysteine conjugate substrate used, the assay method used, and even the laboratory reporting the data. Table 17 summarizes activity data or, when available, kinetic parameters, for β-lyase activity in kidney cytosol or homogenates from rats, mice, and humans. K_m values for cysteine conjugates are, with the exception of two reports, > 1 mM, indicating that the β-lyase is a relatively low-affinity pathway. Activities vary considerably among substrates. In the one study (*157*) where β-lyase activity in kidney cytosol from male and female rats, mice and humans was measured together; the results showed that K_m values for *S*-(1,2,2-trichlorovinyl)-L-cysteine (TCVC) were markedly higher and V_{max} values were markedly lower for mice and humans as compared to rats. This species difference is consistent with the higher susceptibility of

Table 16. Measurements of GGT activity in liver and kidney from male and female F344 rats and B6C3F$_1$ mice and pooled human liver and kidney samples.[a]

Sex	Species	Tissue	Fraction	Activity (mU/mg)
Male	Mouse	Liver	Cytosol	0.07 ± 0.04
			Microsomes	0.05 ± 0.04
		Kidney	Cytosol	1.63 ± 0.85
			Microsomes	92.6 ± 15.6
Female	Mouse	Liver	Cytosol	0.10 ± 0.10
			Microsomes	0.03 ± 0.03
		Kidney	Cytosol	0.79 ± 0.79
			Microsomes	69.3 ± 14.0
Male	Rat	Liver	Cytosol	< 0.02
			Microsomes	< 0.02
		Kidney	Cytosol	< 0.02
			Microsomes	1,570 ± 100
Female	Rat	Liver	Cytosol	< 0.02
			Microsomes	< 0.02
		Kidney	Cytosol	< 0.02
			Microsomes	1,840 ± 40
Male	Human	Liver	Cytosol	8.89 ± 3.58
			Microsomes	29
		Kidney	Cytosol	13.2 ± 1.0
			Microsomes	960 ± 77

[a]GGT activity was measured spectrophotometrically with 1 mM γ-glutamyl-*p*-nitroanilide and glycylglycine as substrates by determining formation of *p*-nitroanilide at 410 nm. Results are the means ± SE of measurements from 6 experiments for rats, 4 experiments for mice, and 3–9 measurements from humans, except for human kidney microsomes, which is the average of 2 measurements. Data reported in (*153,155*).

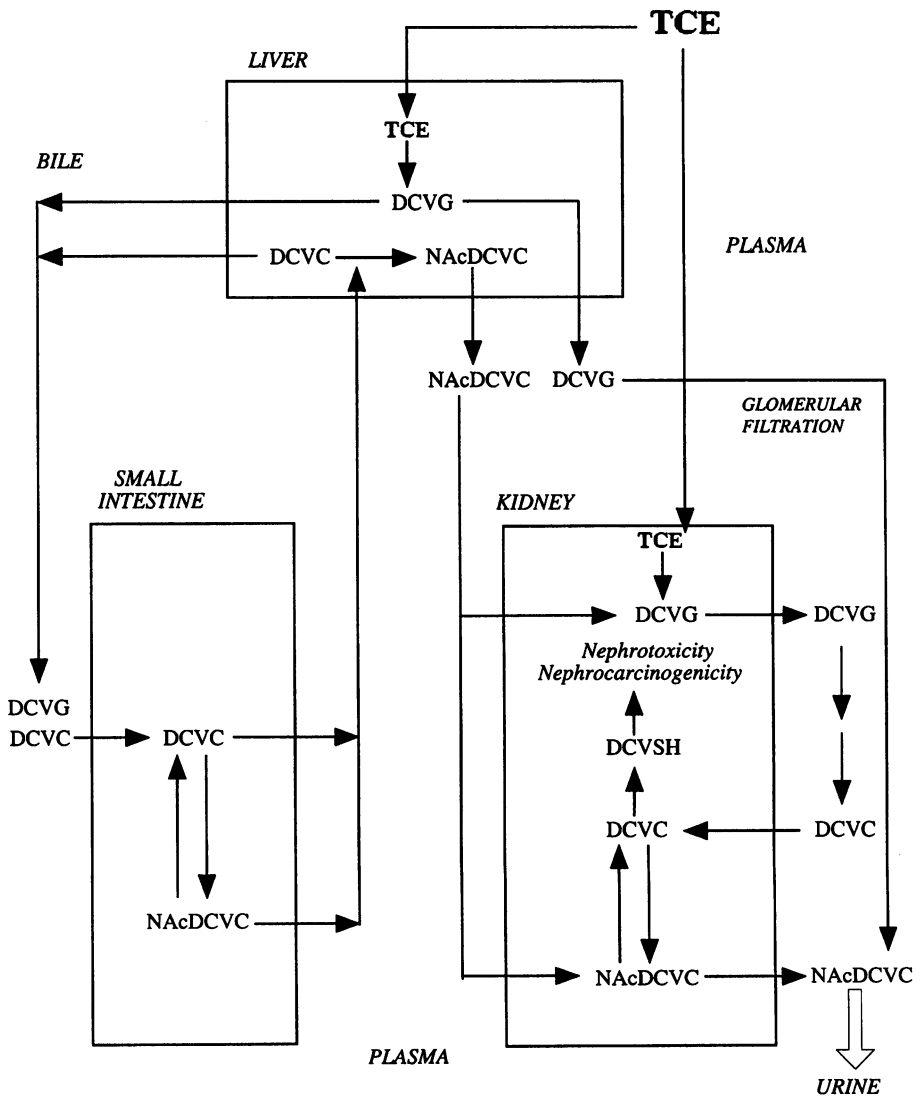

Figure 8. Scheme for interorgan processing and metabolism of TCE by the GSH conjugation pathway.

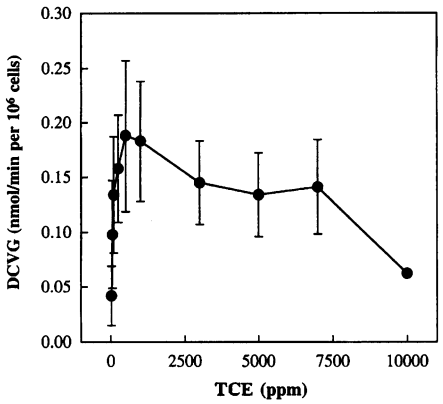

Figure 9. GSH conjugation of TCE in isolated human hepatocytes. Isolated hepatocytes (2.0×10^6 cells/mL) were isolated from livers of human donors and were incubated in sealed flasks with the indicated concentration of TCE in the headspace for 120 min. DCVG formation was assayed in perchloric acid extracts of aliquots of cells by ion-exchange, reversed-phase high-performance liquid chromatography after derivatization with iodoacetate and 1-fluoro-2,4-dinitrobenzene. Derivatives were detected spectrophotometrically at 365 nm and were quantified with respect to authentic standards. Data reported in (*155*).

rats to kidney toxicity and cancer than other species. K_m and V_{max} values for male rats were also lower and higher, respectively, than those for female rats, which is consistent with male rats being more susceptible than female rats. The central questions for risk assessment, therefore, are: *a*) Can studies in male rats be extrapolated to humans? and *b*) Is β-lyase activity in human kidney high enough to generate sufficient amounts of reactive metabolites to produce nephrotoxicity and kidney cancer? Additional studies are clearly necessary to accurately determine flux through this pathway.

Elfarra and Hwang (*158*) used the model cysteine conjugate *S*-(2-benzothiazolyl)-L-cysteine (BTC) as an *in vivo* marker of flux through the β-lyase pathway. BTC was originally synthesized as a convenient assay substrate for the β-lyase (*99*) because it is converted to a stable thiol metabolite, 2-mercaptobenzothiazole (MBT), which can be readily measured spectrophotometrically. They administered BTC to male and female rats and male mice, rats, hamsters, and guinea pigs. BTC is metabolized by the β-lyase and is recovered in the urine as either MBT or MBT glucuronide, both of which are chemically stable and readily measured. Male rats released more metabolite into the urine than female rats and of the four species compared; mice, hamster, and rats excreted comparable levels of total metabolites, whereas the guinea pig excreted more than twice the amount of metabolites as the other species. For the guinea pig, however, the higher excretion rate was not attributable to higher β-lyase activity. Rather, the guinea pig is unique in having extremely low *N*-acetylation activity and extremely high deacetylation activity (*159*), which leads to more BTC being available for β-lyase–mediated metabolism. Hence, measurements of MBT plus MBT glucuronide plus the mercapturate of MBT may provide a useful means of accurately determining flux through the β-lyase pathway.

The importance of *N*-acetylation versus *N*-deacetylation in determining cysteine conjugate nephrotoxicity was highlighted in a recent study by Lau et al. (*159*), in which they determined rates of the forward and reverse reactions for mercapturate formation from *S*-(2,5-dihydroxyphenyl)-L-cysteine, which is a cysteine conjugate derived from

Table 17. Compilation of selected data on cysteine conjugate β-lyase activity from rat, mouse, and human kidney cytosol or homogenates reported in the literature.

Species	Tissue	Substrate	Specific activity (nU/mg protein)	V_{max} (mU/mg protein)	K_m (mM)	Reference
M SD rat	Kidney homogenate	BTC (2 mM)	6.2 ± 1.0			(*99*)
M SD rat	Kidney cytosol	DCVC (1 mM) BTC (1 mM)	3.1 ± 0.2 0.9 ± 0.1			(*108*)
M F344 rat	Kidney cytosol	BTC (0.5 mM)	20.5			(*86*)
M SD rat	Kidney cytosol	DCVC (1 mM; + 0.1 mM KMB)	0.02			(*115*)
M F344 rat	Kidney cytosol	CTFC (4 mM)	22.5 ± 2.5			(*166*)
M F344 rat	Kidney cytosol	BTC CTFC DCVC		74.8 ± 6.5 11.6 ± 1.6 38.3 ± 1.4	1.66 ± 0.19 1.78 ± 0.17 1.36 ± 0.05	(*112*)
M SD rat	Kidney homogenate	DCVC (1 mM; + 0.5 mM KMB)	3.05 ± 0.27			(*111*)
M Wistar rat	Kidney cytosol	DCVC (5 mM) TFEC (5 mM) BTC (1 mM) (+ 0.1 mM KMB)	1.24 2.64 0.70			(*167*)
M F344 rat	Kidney cytosol (purified enzyme) Kidney homogenate	DCVC DCVC (1 mM) PCBC (1 mM)	 4.0 ± 1.0 4.5 ± 0.3	2.2	0.26	(*127*)
M F344 rat	Kidney cytosol	TCVC		4.00 ± 0.11	0.68 ± 0.06	(*157*)
F F344 rat	Kidney cytosol	TCVC		3.64 ± 0.41	1.26 ± 0.21	(*157*)
M B6C3F$_1$ mouse	Kidney cytosol	TCVC		1.15 ± 0.31	5.69 ± 2.22	(*157*)
F B6C3F$_1$ mouse	Kidney cytosol	TCVC		1.66 ± 0.27	4.43 ± 1.42	(*157*)
M human	Kidney cytosol	TCVC		0.49 ± 0.07	2.53 ± 0.09	(*157*)
F human	Kidney cytosol	TCVC		0.64 ± 0.54	2.67 ± 2.11	(*157*)
M human	Kidney cytosol	BTC (2 mM)	0.7			(*113*)
M F344 rat	Kidney cytosol	BTC (2 mM)	6.5			
M Wistar rat	Kidney cytosol	TCVC (0.3 mM)	5.2 ± 0.7			(*168*)
M Wistar rat	Kidney cytosol	DCVC (5 mM; + keto acids)	2.56			(*118*)

Abbreviations: CTFC, *S*-(2-chloro-1,1,2-trifluoroethyl)-L-cysteine; F, female; M, male; PCBC, *S*-(1,2,3,4,4-pentachlorobutadienyl)-L-cysteine; TFEC, *S*-(1,1,2,2-trifluoroethyl)-L-cysteine. Note: Where means ± SE values are shown, data are from 3–7 separate experiments. Where single values are shown, they are from steps during enzyme purification. 1 mU = nmol product formed/min. BTC is a synthetic cysteine conjugate that was developed to assay the β-lyase because it forms a chemically stable thiol metabolite, 2-mercaptobenzothiazole, which can readily be measured spectrophotometrically (*99*).

GSH conjugation of 1,4-benzoquinone, and subsequent metabolism, in several mammalian species. The ratios of *N*-deacetylase to *N*-acetylase activity in these species showed striking differences: F344 and Sprague-Dawley rats exhibited ratios of 0.03 and 0.02, respectively; golden Syrian hamster exhibited a ratio of 0.04, which is similar to that in rats; two mouse strains (BALB/c and B6C3F$_1$) exhibited modestly higher ratios of 0.16 and 0.14, respectively; in contrast to the rat and mouse strains, guinea pigs exhibited a ratio of 4.57. Susceptibility to renal injury at higher doses of the quinone correlated with the ratios in that guinea pigs were the most and rats the least susceptible. At lower doses, however, rats were the most susceptible due to their exceptionally high GGT activity.

Birner et al. (*97*) also assessed deacetylation activity in cytosol from human, Wistar and F344 rat and NMRI mouse kidney using NAcDCVC as the substrate. The rates of deacetylation varied by less than 3-fold across species, varying from 0.35 nmol DCVC formed/min per mg protein in the Wistar rat to values of 0.41, 0.61, and 0.94 in human, F344 rat, and NMRI mouse. They concluded that species-dependent differences in deacetylation activity will influence the amounts of mercapturates recovered in urine.

Variations among Humans

There is much more knowledge about genetic polymorphisms and variations in P450 reactions in humans than there is for GSTs. However, increasing attention is being placed on these potential differences and their toxicological consequences. Analysis of rates of GSH conjugation of TCE in cytosol and microsomes from 20 individual human liver donors has revealed that considerable variation exists (*76*). Overall, rates of GSH conjugation varied 3.4-fold in liver cytosol, exhibiting a range of rates of 28.3–94.9 nmol DCVG formed/20 min per mg protein. The donor pool comprised 9 males and 11 females. There were no significant sex-dependent differences. The liver microsome donors, which comprised 5 males and 15 females, exhibited an overall variation in activity of 8.5-fold, with a range of values from 8.06 to 69.2 nmol DCVG formed per 20 min per mg protein. As with the cytosol donors, there were no significant sex-dependent difference in the mean activity values, although the degree of variation was greater in the females (7.4-fold) than in the males (4.1-fold). Hence, although the degree of variation in GST activity (3- to 8-fold) is significantly less than that observed with P450 activity (10- to 20-fold), this may be another important factor to account for in a human health risk assessment for TCE.

Extrapolation of Experimental Data for Human Health Risk Assessment

Extrapolation from Animals to Humans

A major issue in the extrapolation of experimental metabolism data from animals to humans involves the concentrations of toxicants used. Animal studies often use relatively high concentrations of chemicals that are severalfold to several orders of magnitude higher than those to which humans may be exposed either occupationally or environmentally. This, of course, brings into question the relevance of such data. Examples of a number of species-dependent differences in TCE metabolism have been cited above.

Lipscomb et al. (*66*) recently addressed this specific issue by characterizing the kinetics and P450 isoform specificity of TCE metabolism to CH in liver microsomes from rats, mice, and humans using a full range of concentrations of TCE, including those that are estimated to occur in the livers of some occupationally exposed humans. Analysis of the kinetics of TCE metabolism to CH showed that rats metabolized TCE very differently than either mice or humans: Rat liver microsomes exhibited at least three kinetically distinct processes for TCE metabolism, whereas mouse and human liver exhibited only a single process. Human liver microsomes exhibited similar overall K_m values for TCE as those from rats or mice but had markedly (3- to 8-fold) lower V_{max} values. Hence, different kinetic behavior among experimental animal species and humans must be considered when extrapolating animal data.

Extrapolation from *in Vitro* to *in Vivo*

The other most common type of extrapolation performed is from *in vitro* data to the *in vivo* situation. This is particularly important for humans as most of our data come from biopsy tissue samples, cell lines, or tissue obtained from hospitals where the tissue cannot be used for transplant. One simple issue is how to use data from liver microsomes or isolated hepatocytes to quantitate metabolism at the level of the entire organ or organism. This process uses what have been called scaling factors, and data from two studies are summarized (Table 18).

Lipscomb et al. (*11*) calculated parameters that enable one to extrapolate to whole liver in humans from measurements made in isolated hepatocytes or suspensions of microsomes. The parameters express the number of hepatocytes per gram of liver, the amount of microsomal protein per gram of liver, and the amount of microsomal protein in a suspension of hepatocytes. Carlile et al. (*160*) made similar use of scaling factors in studies with rats to relate rates of drug metabolism in various *in vitro* systems to rates in whole liver.

Kedderis (*161*) raised an important caveat in the extrapolation of *in vitro* data to the *in vivo* situation. Using enzyme induction as a model, Kedderis showed that pretreatment with inducers may significantly increase rates of drug metabolism *in vitro* but that physiological constraints may dampen these effects *in vivo*. He cites the example of furan metabolism, which is catalyzed by CYP2E1. Severalfold variations were observed in the bioactivation of the hepatotoxicant furan by isolated human hepatocytes owing to variations in this P450 isoform in the human population. Extrapolation of these data to the *in vivo* situation showed that furan metabolism is limited by hepatic blood flow. Because of this limitation, variations in CYP2E1 content among individual liver donors and increases in V_{max} due to inducers will be markedly dampened *in vivo*.

Relative Roles of Oxidative and GSH Conjugation Pathways in TCE Metabolism

A principal issue in understanding the relative roles of the two major pathways of TCE metabolism is that of pathway affinity. Based on known kinetic parameters of TCE metabolism, relative rates of oxidative metabolism and GSH conjugation under different exposure conditions (i.e., acute or chronic high

Table 18. Parameters used to extrapolate from microsomes and isolated hepatocytes to whole liver in humans.

Parameter	Value
Human liver[a]	
Hepatocyte density	116×10^6 cells/g liver
Microsomal protein density: whole liver	20.88 mg microsomal protein/g liver
Microsomal protein density: isolated cells	179 µg microsomal protein/10^6 cells
Rat liver[b]	
DNA content of liver	2.6–2.7 mg DNA/g liver
DNA content of hepatocytes	21.5–26.8 µg DNA/10^6 cells
Hepatocyte density (based on DNA data)	$73–94 \times 10^6$ cells/g liver
Protein[c] content of liver	163–176 mg/g liver
Protein[c] content of cells	1.4–1.5 mg protein/10^6 cells
Hepatocyte density (based on protein data)	$109–125 \times 10^6$ cells/g liver

[a]Data are from (*11*). [b]Data are from Carlile et al. (*160*) and involve animals that have been treated with inducers of various P450s. [c]Total cellular protein, not just microsomal protein.

doses versus chronic low doses, such as those found as environmental contaminants) can be determined. From this information, the predominance of different metabolites at various doses can be discerned. Moreover, knowledge of which metabolic pathway predominates at specific doses can help determine target organ specificity and mode of action at those doses. Additionally, the two major pathways of TCE metabolism are known to have markedly different kinetics, so that they saturate at different doses. Hence, the relative proportion of metabolites formed will likely vary markedly at low versus high doses. Specifically, CYP2E1 saturates at significantly lower doses of TCE than do the GSTs, suggesting that flux of TCE through the GSH conjugation pathway may only be quantitatively important at higher doses of TCE. As mentioned earlier, however, the GSH conjugation pathway, and specifically the β-lyase reaction, generates chemically reactive metabolites; formation of even a small amount of a reactive species may be sufficient to produce alterations in cellular function whereas formation of relatively large amounts of a non-reactive metabolite may not produce any cellular dysfunction.

Hence, although one may conclude by intuition that a low-affinity pathway may only be of toxicological importance at high doses and/or when the high-affinity pathway is saturated, this is not necessarily correct for a pathway such as that catalyzed by the β-lyase that generates chemically unstable and reactive metabolites. It has been argued that the β-lyase pathway is not quantitatively important for humans, based on the following points: *a*) Kinetic parameters (i.e., affinity and capacity) of the β-lyase in human kidney, as compared to those for P450 oxidation in human liver, are such that β-lyase activity will only become quantitatively significant at extremely high exposure levels; *b*) TCE exposure studies comparing excretion of mercapturate to that of TCA and TCOH show that the P450-derived metabolites are recovered in urine at levels that are two to three orders of magnitude higher than the GSH-derived metabolite; and *c*) questions have arisen about the relevance of reports of kidney tumors in human populations exposed to TCE. I will discuss the first two points below. The third point will be only briefly discussed, as this is dealt with in greater detail in the kidney mode of action review (*89*).

Concerning the first point about the relative kinetic parameters of the oxidative and GSH conjugation pathways, there is no doubt that flux through the P450 pathway is much faster and that the total capacity is much greater than for the GSH conjugation and β-lyase reactions. There are two major differences between the nature of the metabolites formed by the two pathways. First, the various enzymes of the GSH conjugation pathway and the membrane transporters for GSH and cysteine conjugates and mercapturates exhibit significant tissue heterogeneity so that metabolites are directed to the kidneys for intracellular accumulation and metabolism to reactive species. Second, the metabolites from the GSH conjugation pathway that are believed to be responsible for effects in the kidneys are chemically unstable and highly reactive whereas those derived from the oxidative pathway are relatively stable. Because of the nature of reactive metabolites, it is likely that relatively small amounts of these compounds can produce significant biochemical and functional changes in renal cells. One cannot, therefore, directly extrapolate from amount of metabolite formed or pathway flux to toxicity.

Concerning the second point about recovery of mercapturates compared to the recovery of TCA and TCOH in the urine, two types of exposures were conducted by Henschler's group (*96,97*) that show the variability in recovery of excreted metabolites with exposure route (Table 19). However, even in the studies that show lower ratios of oxidative metabolites (TCA or TCA + TCOH) to NAcDCVC, it has been argued that ratios as little as 10:1 indicate that the flux through the GSH conjugation pathway is at least an order of magnitude slower than that through P450. It must be emphasized, however, that measurement of urinary mercapturate provides only an indication of a portion of the GSH-dependent pathway and that this portion is not related to that which is associated with nephrotoxicity and nephrocarcinogenicity. Measurement of urinary mercapturates, therefore, can give an indication of exposure and that some flux through the GSH conjugation pathway has occurred. It cannot, however, give an indication of total flux through the GSH conjugation pathway or through that portion of the pathway that leads to effects on renal function. Moreover, formation of even a small amount of reactive species may be sufficient to produce toxic effects or changes in intracellular regulatory mechanisms.

Concerning the third point about the occurrence of kidney tumors being much lower than those in the other target organs and this relating to a small flux through the GSH conjugation and β-lyase pathways, the following points should be noted: *a*) the background rate of kidney tumors is extremely small in humans and most animal species studied (although some strains of rats show a relatively high background rate); *b*) the kidneys are particularly susceptible to cytotoxic injury from even brief, low-dose exposures to nephrotoxicants; and *c*) proximal tubular epithelial cells can undergo a program of apoptosis and regeneration after exposures to sublethal doses, or even necrotic doses, of nephrotoxicants. These points should highlight the difficulties in assessment of factors involved in induction of renal carcinogenesis.

Although species- and sex-dependent differences are found in various steps of TCE metabolism, it is important to also consider the entire pathway as a whole and not just individual reactions. Although the rate of a specific step may be relevant to a consideration of toxicity if the toxicity is solely dependent on the formation of a specific metabolite, the balance between metabolite formation and subsequent metabolic steps and species differences in the ratio of these steps are often of more importance.

In summary, it is clear that the oxidative pathway is quantitatively the more important of the two major pathways of TCE metabolism. However, the interorgan patterns of the GSH-dependent pathway and the chemical nature of the critical metabolites generated by the two pathways greatly alters the importance of simple comparisons of quantitation. Furthermore, we do not really have an accurate method to assess flux through all branches of the GSH-dependent pathway because chemically reactive species are generated.

Table 19. Summary of studies on mercapturate and oxidative metabolite excretion in urine of rats, mice, and humans exposed to TCE.

Study I: Exposure of Wistar rats and NMRI mice to TCE 22 hr after exposure (50 mg/kg by oral gavage) (*97*)

Sex/species	TCA/NAcDCVC in urine
Male rat	22.0
Female rat	39.4
Male mouse	15.3
Female mouse	72.5

Study II: Exposure of workers to TCE by inhalation or dermal contact (*97*).

Worker number	TCA/NAcDCVC in urine
1	18.5
5	17.9
6	3.1
8	32.8

Study III: Exposure of humans and male and female Wistar rats to TCE (6-hr inhalation). Cumulative excretion of metabolites measured over 48 hr post-exposure (*96*).

Species	[TCE] in exposure chamber	(TCA + TCOH)/ NAcDCVC
Human	40 ppm	3,292
	80 ppm	4,797
	160 ppm	7,163
Rat	40 ppm	986
	80 ppm	1,300
	160 ppm	2,562

Questions and Research Needs

This section briefly discusses some key research needs in the area of TCE metabolism. Although study of these questions is not, in most cases, essential to completion of an updated human health risk assessment for TCE, research on these questions will answer important questions and address uncertainties that will improve our understanding of TCE metabolism.

Role of an Epoxide Intermediate in TCE Metabolism

The question of whether TCE, like many other halogenated solvents that undergo P450-dependent metabolism, does so through intermediate formation of an epoxide is still uncertain and should be resolved by careful chemical studies.

Enzymology of DCA Formation

Two issues regarding amounts of and sources of DCA formation are still incompletely resolved. The first issue relates to the recovery of DCA in biological incubations with TCE, as questions remain about the recovery of DCA in tissue incubations and biological fluids such as plasma and urine. The second issue relates to the sources of and specific enzymes involved in DCA formation. It is unclear what factors determine how much of DCA is derived from TCA, TCOH, or CH and what the specific involvement is of enzymes such as P450s or aldehyde dehydrogenase.

P450 Isoform Activity Distribution

Although CYP2E1 has been identified as the most active P450 isoform responsible for oxidative metabolism of TCE, questions remain about the potential activities of other isoforms, both in uninduced and in induced individuals. Expression of many P450 isoforms exhibits sex and species differences. These differences, specifically in relation to TCE metabolism, need to be more completely assessed as various physiological or pathological changes in P450 isoform activity distribution can alter metabolism and susceptibility to toxicity. Unequivocal identification of the role of specific isoforms will require the use of inhibitory antibodies and studies with expressed and purified enzymes.

Role of Renal P450 in TCE Metabolism and Bioactivation

Little investigation of renal P450 activities in comparison to hepatic P450s has been undertaken. Although many of the same isoforms as are found in the liver have been identified in the kidneys, their regulation may be different in the two organs. For example, many of the known inducers of hepatic CYP2E1 do not have the same qualitative or quantitative effects on renal CYP2E1. Based on the knowledge that CYP2E1 is active in TCE oxidation, this differential regulation should impact on oxidative metabolism of TCE in the kidneys.

Almost all of the focus of TCE metabolism in the kidneys has been on the GSH-dependent pathway. Although there is no direct evidence to suggest that intrarenal formation of metabolites such as TCA or DCA is involved in the renal effects of TCE, this issue has not been investigated fully so we should not a priori rule it out.

GST Isozyme Distribution and Variation

Recent work has revealed that the various GSTs exist in isozymic forms and that sex-, species-, and tissue-dependent differences often exist. The substrate specificity of these isozymes and specifically the activity of each isozyme toward TCE is unknown at present. Brüning et al. (*162*) have recently shown that genetic polymorphisms exist in two GSTs, GSTM1 and GSTT1, and that differences in expression of these isozymes may have toxicological significance for TCE bioactivation by this pathway. Hence, work is needed to define the isozyme composition in various species, including humans, and in various tissues in each species, and to define the activity of each isozyme towards TCE.

Quantitative Importance of DCVC Metabolism in Humans

The difficulties in assessing the quantitative importance of flux through the GSH conjugation pathway, and through the β-lyase reaction specifically, have been discussed above in some detail. Three key issues are

- Improved measurements of overall flux of TCE through the GSH conjugation pathway and the β-lyase as compared to that through the oxidative pathway by more complete determinations of rates of metabolism and kinetic parameters in tissues from various species, particularly humans.
- Development of more accurate, noninvasive means of measuring flux through the β-lyase pathway in humans. Urinary mercapturates only provide information on stable end products and these do not necessarily correlate with formation of reactive metabolites that produce nephrotoxicity and/or nephrocarcinogenicity.
- Data on formation of covalent adducts of DCVC with DNA and protein have been difficult to interpret and may not directly correspond to cytotoxic or tumorigenic events. Hence, additional studies on the functional significance of covalent binding to cellular macromolecules are warranted.

References and Notes

1. Wu C, Becker J, Schaum J. Major findings of the exposure assessment of trichloroethylene and related compounds. Environ Health Perspect 108(supp 2):359–358 (2000).
2. Clewell HJ III, Gentry PR, Covington TR, Gearhart JM. Development of a physiologically based pharmacokinetic model of trichloroethylene and its metabolites for use in risk assessment. Environ Health Perspect 108(suppl 2):283–305 (2000).
3. Sato A, Nakajima T. Differences following skin or inhalation exposure in the absorption and excretion kinetics of trichloroethylene and toluene. Br J Ind Med 35:43–49 (1978).
4. Davidson IWF, Beliles RP. Consideration of the target organ toxicity of trichloroethylene in terms of metabolite toxicity and pharmacokinetics. Drug Metab Rev 23:493–599 (1991).
5. Bogen KT, Colston BW Jr, Machicao LK. Dermal absorption of dilute aqueous chloroform, trichloroethylene, and tetrachloroethylene in hairless guinea pigs. Fundam Appl Toxicol 18:30–39 (1992).
6. Withey JR, Collins BT, Collins PG. Effect of vehicle on the pharmacokinetics and uptake of four halogenated hydrocarbons from the gastrointestinal tract of the rat. J Appl Toxicol 3:249–253 (1983).
7. Prout MS, Provan WM, Green T. Species differences in response to trichloroethylene. I: Pharmacokinetics in rats and mice. Toxicol Appl Pharmacol 79:389–400 (1985).
8. Fisher JW, Gargas ML, Allen BC, Andersen ME. Physiologically based pharmacokinetic modeling with trichloroethylene and its metabolite, trichloroacetic acid, in the rat and mouse. Toxicol Appl Pharmacol 109:183–195 (1991).
9. Bull RJ. Mode of action of liver tumor induction by trichloroethylene. Environ Health Perspect 108(supp 2):241–259(2000).
10. Dallas CE, Gallo JM, Ramanathan R, Muralidhara S, Bruckner JV. Physiological pharmacokinetic modeling of inhaled trichloroethylene in rats. Toxicol Appl Pharmacol 110:303–314 (1991).
11. Lipscomb JC, Fisher JW, Confer PD, Byczkowski JZ. In vitro to in vivo extrapolation for trichloroethylene metabolism. Toxicol Appl Pharmacol 152:376–387 (1998).
12. Daniel JW. The metabolism of ^{36}Cl-labeled trichloroethylene and tetrachloroethylene in the rat. Biochem Pharmacol 12:795–802 (1963).
13. Dekant W, Metzler M, Henschler D. Novel metabolites of trichloroethylene through dechlorination reactions in rats, mice and humans. Biochem Pharmacol 33:2021–2027 (1984).
14. D'Souza RW, Bruckner JV, Feldman S. Oral and intravenous trichloroethylene pharmacokinetics in the rat. J Toxicol Environ Health 15:587–601 (1985).
15. Lee K, Bruckner JV, Muralidhara S, Gallo JM. Characterization of presystemic elimination of trichloroethylene and its nonlinear kinetics in rats. Toxicol Appl Pharmacol 139:262–271 (1996).
16. Kleinfeld M, Tabershaw IR. Trichloroethylene toxicity: report of five fatal cases. Arch Ind Hyg Occup Med 10:134–141 (1954).
17. Brüning T, Vamvakas S, Makropoulos V, Birner G. Acute intoxication with trichloroethene: clinical symptoms, toxicokinetics, metabolism, and development of biochemical parameters for renal damage. Toxicol Sci 41:157–165 (1998).
18. Allen BC, Fisher JW. Modeling of the pharmacokinetics of trichloroethylene and trichloroacetic acid in humans. Risk Anal 13:71–86 (1993).
19. Fisher JW, Mahle D, Abbas R. A human physiologically-based pharmacokinetic model for trichloroethylene and its metabolites, trichloroacetic acid and free trichloroethanol. Toxicol Appl Pharmacol 152:339–359 (1998).
20. Fisher JW, Whittaker TA, Taylor DH, Clewell HJ III, Andersen ME. Physiologically-based pharmacokinetic modeling of the pregnant rat: a multiroute exposure model for trichloroethylene and its metabolite, trichloroacetic acid. Toxicol Appl Pharmacol 99:395–414 (1989).
21. Müller G, Spassovski M, Henschler D. Trichloroethylene exposure and trichloroethylene metabolites in urine and blood. Arch Toxicol 29:335–340 (1972).
22. Abbas R, Fisher JW. A physiologically-based pharmacokinetic model for trichloroethylene and its metabolites, chloral hydrate, trichloroacetate, dichloroacetate, trichloroethanol, and trichloroethanol glucuronide in B6C3F1 mice. Toxicol Appl Pharmacol 147:15–30 (1997).
23. Anders MW, Jakobson I. Biotransformation of halogenated solvents. Scand J Work Environ Health 11(suppl 1):23–32 (1985).
24. Butler TC. Metabolic transformations of trichloroethylene. J Pharmacol Exp Ther 97:84–92 (1949).
25. Powell JF. Trichloroethylene: absorption, elimination and metabolism. Br J Ind Med 2:142–145 (1945).
26. Miller RE, Guengerich FP. Oxidation of trichloroethylene by liver

microsomal cytochrome P-450: evidence for chlorine migration in a transition state not involving trichloroethylene oxide. Biochemistry 21:1090–1097 (1982).
27. Miller RE, Guengerich FP. Metabolism of trichloroethylene in isolated hepatocytes, microsomes, and reconstituted systems containing cytochrome P-450. Cancer Res 43:1145–1152 (1983).
28. Green T, Prout MS. Species differences in response to trichloroethylene. II: Biotransformation in rats and mice. Toxicol Appl Pharmacol 79:401–411 (1985).
29. Dowsley TF, Ulreich JB, Bolton JL, Park SS, Forkert PG. CYP2E1-dependent bioactivation of 1,1-dichloroethylene in murine lung: formation of reactive intermediates and glutathione conjugates. Toxicol Appl Pharmacol 139:42–48 (1996).
30. Forkert PG. In vivo formation and localization of 1,1-dichloroethylene epoxide in murine liver: identification of its glutathione conjugate 2-*S*-glutathionyl acetate. J Pharmacol Exp Ther 290:1299–1306 (1999).
31. Forkert PG. 1,1-Dichloroethylene-induced Clara cell damage is associated with in situ formation of the reactive epoxide. Immunohistochemical detection of its glutathione conjugate. Am J Respir Cell Mol Biol 20:1310–1318 (1999).
32. Forkert PG, Malkinson AM, Rice P, Moussa M. Diminished CYP2E1 expression and formation of 2-*S*-glutathionyl acetate, a glutathione conjugate derived from 1,1-dichloroethylene epoxide, in murine lung tumors. Drug Metab Dispos 27:68–73 (1999).
33. U.S. EPA. Health Assessment Document for Trichloroethylene. Final Report. Office of Health and Environmental Assessment. EPA/600/8-82-006F, Washington, DC:U.S. Environmental Protection Agency, 1985.
34. Goeptar AR, Commandeur JNM, van Ommen B, van Bladeren PJ, Vermeulen NPE. Metabolism and kinetics of trichloroethylene in relation to toxicity and carcinogenicity. Relevance of the mercapturic acid pathway. Chem Res Toxicol 8:3–21 (1995).
35. Guengerich FP. Oxidation of toxic and carcinogenic chemicals by human cytochrome P-450 enzymes. Chem Res Toxicol 4:391–407 (1991).
36. Guengerich FP, Kim D-H, Iwasaki M. Role of human cytochrome P-450 IIE1 in the oxidation of many low molecular weight cancer suspects. Chem Res Toxicol 4:168–179 (1991).
37. Koop DR, Crump BL, Nordblom GD, Coon MJ. Immunochemical evidence for induction of the alcohol-oxidizing cytochrome P-450 of rabbit liver microsomes by diverse agents: ethanol, imidazole, trichloroethylene, acetone, pyrazole, and isoniazid. Proc Natl Acad Sci USA 82:4065–4069 (1985).
38. Nakajima T, Okino T, Okuyama S, Kaneko T, Yonekura I, Sato A. Ethanol-induced enhancement of trichloroethylene metabolism and hepatotoxicity: difference from the effect of phenobarbital. Toxicol Appl Pharmacol 94:227–237 (1988).
39. Nakajima T, Wang R-S, Murayama N, Sato A. Three forms of trichloroethylene-metabolizing enzymes in rat liver induced by ethanol, phenobarbital, and 3-methylcholanthrene. Toxicol Appl Pharmacol 102:546–552 (1990).
40. Nakajima T, Wang R-S, Elovaara R, Park SS, Gelboin HV, Vainio H. A comparative study on the contribution of cytochrome P450 isozymes to metabolism of benzene, toluene and trichloroethylene in rat liver. Biochem Pharmacol 43:251–257 (1992).
41. Nakajima T, Wang R-S, Katakura Y, Kishi R, Elovaara E, Park SS, Gelboin HV, Vainio H. Sex-, age- and pregnancy-induced changes in metabolism of toluene and trichloroethylene in rat liver in relation to the regulation of cytochrome P450IIE1 and P450IIC11 content. J Pharmacol Exp Ther 261:869–874 (1992).
42. Nakajima T, Wang R-S, Elovaara E, Park SS, Gelboin HV, Vainio H. Cytochrome P450-related differences between rats and mice in the metabolism of benzene, toluene and trichloroethylene in liver microsomes. Biochem Pharmacol 45:1079–1085 (1993).
43. Forkert PG, Birch DW. Pulmonary toxicity of trichloroethylene in mice: covalent binding and morphological manifestations. Drug Metab Dispos 17:106–113 (1989).
44. Green T, Mainwaring GW, Foster JR. Trichloroethylene-induced mouse lung tumors: studies of the mode of action and comparisons between species. Fundam Appl Toxicol 37:125–130 (1997).
45. Odum J, Foster JR, Green T. A mechanism for the development of Clara cell lesions in the mouse lung after exposure to trichloroethylene. Chem-Biol Interact 83:135–153 (1992).
46. Abbas R, Seckel CS, Kidney JK, Fisher JW. Pharmacokinetic analysis of chloral hydrate and its metabolism in B6C3F1 mice. Drug Metab Dispos 24:1340–1346 (1996).
47. Larson LJ, Bull RJ. Effect of ethanol on the metabolism of trichloroethylene. J Toxicol Environ Health 28:395–406 (1989).
48. Müller G, Spassovski M, Henschler D. Metabolism of trichloroethylene in man. III: Interaction of trichloroethylene and ethanol. Arch Toxicol 33:173–189 (1975).
49. Ni Y-C, Wong T-Y, Lloyd RV, Heinze TM, Shelton S, Casciano D, Kadlubar FF, Fu PP. Mouse liver microsomal metabolism of chloral hydrate, trichloroacetic acid, and trichloroethanol leading to induction of lipid peroxidation via a free radical mechanism. Drug Metab Dispos 24:81–90 (1996).
50. Schultz J, Weiner H. Alteration of the enzymology of chloral hydrate reduction in the presence of ethanol. Biochem Pharmacol 28:3379–3384 (1979).
51. Sellers EM, Lang M, Koch-Weser J, LeBlanc E, Kalant H. Interaction of chloral hydrate and ethanol in man. I: Metabolism. Clin Pharmacol Ther 13:37–49 (1972).
52. Lipscomb JC, Mahle DA, Brashear WT, Garrett CM. A species comparison of chloral hydrate metabolism in blood and liver. Biochem Biophys Res Commun 227:340–350 (1996).
53. Dekant W, Schulz A, Metzler M, Henschler D. Absorption, elimination and metabolism of trichloroethylene: a quantitative comparison between rats and mice. Xenobiotica 16:143–152 (1986).
54. Larson JL, Bull R.J. Species differences in the metabolism of trichloroethylene to the carcinogenic metabolites trichloroacetate and dichloroacetate. Toxicol Appl Pharmacol 115:278–285 (1992).
55. Templin MV, Stevens DK, Stenner RD, Bonate PL, Tuman D, Bull RJ. Factors affecting species differences in the kinetics of metabolites of trichloroethylene. J Toxicol Environ Health 44:435–447 (1995).
56. Larson JL, Bull RJ. Metabolism and lipoperoxidative activity of trichloroacetate and dichloroacetate in rats and mice. Toxicol Appl Pharmacol 115:268–277 (1992).
57. Templin MV, Parker JC, Bull RJ. Relative formation of dichloroacetate and trichloroacetate from trichloroethylene in male B6C3F1 mice. Toxicol Appl Pharmacol 123:1–8 (1993). [Erratum published in Toxicol Appl Pharmacol 133:177 (1995)]
58. Ketcha MM, Stevens DK, Warren DA, Bishop CT, Brashear WT. Conversion of trichloroacetic acid to dichloroacetic acid in biological samples. J Anal Toxicol 20:236–241 (1996).
59. Henderson GN, Yan Z, James MO, Davydova N, Stacpoole PW. Kinetics and metabolism of chloral hydrate in children: Identification of dichloroacetate as a metabolite. Biochem Biophys Res Commun 235:695–698 (1997).
60. Lipscomb JC, Mahle DA, Brashear WT, Barton HA. Dichloroacetic acid: metabolism in cytosol. Drug Metab Dispos 23:1202–1205 (1995).
61. James MO, Cornett R, Yan Z, Henderson GN, Stacpoole PW. Glutathione-dependent conversion to glyoxylate, a major pathway of dichloroacetate biotransformation in hepatic cytosol from humans and rats, is reduced in dichloroacetate-treated rats. Drug Metab Dispos 25:1223–1227 (1997).
62. Tong Z, Board P, Anders MW. Glutathione transferase zeta catalyzes the oxygenation of the carcinogen dichloroacetic acid to glyoxylic acid. Biochem J 331:371–374 (1998).
63. Cummings BS, Putt DW, Parker JC, Lash LH. Unpublished data.
64. Lipscomb JC, Garrett CM, Snawder JE. Cytochrome P450 dependent metabolism of trichloroethylene: interindividual differences in humans. Toxicol Appl Pharmacol 142:311–319 (1997).
65. Wrighton SA, Stevens JC. The human hepatic cytochromes P450 involved in drug metabolism. CRC Crit Rev Toxicol 22:1–21 (1992).
66. Lipscomb JC, Garrett CM, Snawder JE. Use of kinetic and mechanistic data in species extrapolation of bioactivation: cytochrome P-450 dependent trichloroethylene metabolism at occupationally relevant concentrations. J Occup Health 40:110–117 (1998).
67. Moghaddam AP, Abbas R, Fisher JW, Stavrou S, Lipscomb JC. Metabolism of trichloroacetic acid to dichloroacetic acid by rat and mouse gut microflora, an in vitro study. Biochem Biophys Res Commun 228:639–645 (1996).
68. Moghaddam AP, Abbas R, Fisher JW, Lipscomb JC. Role of mouse intestinal microflora in dichloroacetic acid formation, an in vivo study. Human Exp Toxicol 16:629–635 (1997).
69. Maiorino RM, Gandolfi AJ, Sipes IG. Gas chromatographic method for the halothane metabolites, trifluoroacetic acid and bromide, in biological fluids. Anal Toxicol 4:250–254 (1980).
70. Elfarra AA, Krause RJ, Last LR, Lash LH, Parker JC. Species- and sex-related differences in metabolism of trichloroethylene to yield chloral and trichloroethanol in mouse, rat, and human liver microsomes. Drug Metab Dispos 26:779–785 (1998).
71. Peter R, Bocker R, Beaune PH, Iwasaki M, Guengerich FP, Yang CS. Hydroxylation of chlorzoxazone as a specific probe for human liver cytochrome P450 IIE1. Chem Res Toxicol 3:566–573 (1990).
72. Shimada T, Yamazaki H, Mimura M, Inui Y, Guengerich FP. Interindividual variations in human liver cytochrome P450 enzymes involved in the oxidation of drugs, carcinogens, and toxic chemicals. Studies with liver microsomes of 30 Japanese and 30 Caucasians. J Pharmacol Exp Ther 270:414–423 (1994).
73. Barton HA, Flemming CD, Lipscomb JC. Evaluating human variability in chemical risk assessment: hazard identification and dose-response assessment for noncancer oral toxicity of trichloroethylene. Toxicology 110:271–287 (1996).
74. Lindahl R, Evces S. Comparative subcellular distribution of aldehyde dehydrogenase in rat, mouse and rabbit liver. Biochem Pharmacol 33:3383–3389 (1984).
75. Badawy AA, Aliyu SU. Antagonism of acute alcohol intoxication by naloxone. Alcohol 19:199–201 (1984).
76. Lipscomb JC. Unpublished data.
77. Sellers EM, Lang-Sellers M, Koch-Weser J. Comparative metabolism of chloral hydrate and trichlofos. J Clin Pharmacol 18:457–461 (1978).
78. Pravecek TL, Channel SR, Schmidt WJ, Kidney JK. Cytotoxicity and metabolism of dichloroacetic acid and trichloroacetic acid in B6C3F1 mouse liver tissue. In Vitro Toxicology 9:261–269 (1996).
79. Kawamoto T, Hobara T, Aoki T, Kobayashi H, Iwamoto S, Sakai T, Miyazaki Y, Imamura A, Ogino K. Metabolism of chloral hydrate in the anoxic perfused liver. Toxicol Lett 40:225–231 (1988).
80. Wang GZ, Takano T, Tomita T, Nakata K, Nakamura K. Interaction of trichloroethylene and isopropyl alcohol in the perfused rat liver. Nippon Eiseigaku Zasshi 48:1000–1005 (1993).
81. Reitz RH, Garagas ML, Mendrala AL, Schumann AM. In vivo and in vitro studies of perchloroethylene metabolism for physiologically-based pharmacokinetic modeling in rats, mice and humans. Toxicol Appl Pharmacol 136:289–306 (1996).
82. McKinney LL, Weakley FB, Eldridge AC, Campbell RG, Cowan JC, Beister HW. *S*-(Dichlorovinyl)-L-cysteine: an agent causing fatal aplastic anemia in calves. J Am Chem Soc 79:3932–3933 (1957).
83. McKinney LL, Picken JC, Weakley FB, Eldridge AC, Campbell RG, Cowan JC, Beister HE. Possible toxic factor of trichloroethylene-extracted soybean oil. J Am Chem Soc 81:909–915 (1959).
84. Dekant W, Metzler M, Henschler D. Identification of *S*-(1,2-dichlorovinyl)-*N*-acetyl-cysteine as a urinary metabolite of trichloroethylene: a possible explanation for its nephrocarcinogenicity in male rats. Biochem Pharmacol 35:2455–2458 (1986).
85. Elfarra AA, Anders MW. Renal processing of glutathione conjugates: role in nephrotoxicity. Biochem Pharmacol 33:3729–3732 (1984).
86. Elfarra AA, Jakobson I, Anders MW. Mechanism of *S*-(1,2-dichlorovinyl)glutathione-induced nephrotoxicity. Biochem Pharmacol 35:283–288 (1986).
87. Dekant W, Koob M, Henschler D. Metabolism of trichloroethene — In vivo and in vitro evidence for activation by glutathione conjugation. Chem-Biol Interact 73:89–101 (1990).
88. Lash LH, Putt DA, Brashear WT, Abbas R, Parker JC, Fisher JW. Identification of *S*-(1,2-dichlorovinyl)glutathione in the blood of human volunteers exposed to trichloroethylene. J Toxicol Environ Health 56:1–21 (1999).
89. Lash LH, ParkerJC, Scott CS. Modes of action of trichloroethylene for kidney tumorigenesis. Environ Health Perspect 108(suppl 2):225–240 (2000).
90. Lash LH, Jones DP, Anders MW. Glutathione homeostasis and glutathione *S*-conjugate toxicity in kidney. Rev Biochem Toxicol 9:29–67 (1988).
91. Lash LH, Anders MW. Cytotoxicity of *S*-(1,2-dichlorovinyl)glutathione and *S*-(1,2-dichlorovinyl)-L-cysteine in isolated rat kidney cells. J Biol Chem 261:13076–13081 (1986).
92. Duffel MW, Jakoby WB. Cysteine *S*-conjugate *N*-acetyltransferase from rat kidney microsomes. Mol Pharmacol 21:444–448 (1982).
93. Wolfgang GH, Gandolfi AJ, Stevens JL, Brendel K. *N*-Acetyl-*S*-(1,2-dichlorovinyl)-L-cysteine produces a similar toxicity to *S*-(1,2-dichlorovinyl)-L-cysteine in rabbit renal slices: differential transport and metabolism. Toxicol Appl Pharmacol 101:205–219 (1989).
94. Zhang G, Stevens JL. Transport and activation of *S*-(1,2-dichlorovinyl)-L-cysteine and *N*-acetyl-*S*-(1,2-dichlorovinyl)-L-cysteine in rat kidney proximal tubules. Toxicol Appl Pharmacol 100:51–61 (1989).
95. Commandeur JNM, Vermeulen NPE. Identification of *N*-acetyl(2,2-dichlorovinyl)- and *N*-acetyl(1,2-dichlorovinyl)-L-cysteine as two regioisomeric mercapturic acids of trichloroethylene in the rat. Chem Res Toxicol 3:212–218 (1990).
96. Bernauer U, Birner G, Dekant W, Henschler D. Biotransformation of trichloroethene: dose-dependent excretion of 2,2,2-trichloro-metabolites and mercapturic acids in rats and humans after inhalation. Arch Toxicol 70:338–346 (1996).
97. Birner G, Vamvakas S, Dekant W, Henschler D. Nephrotoxic and genotoxic *N*-acetyl-*S*-dichlorovinyl-L-cysteine is a urinary metabolite after occupational 1,1,2-trichloroethene exposure in humans: implications for the risk of trichloroethene exposure. Environ Health Perspect 99:281–284 (1993).

98. Anderson PM, Schultze MO. Cleavage of *S*-(1,2-dichlorovinyl)-L-cysteine by and enzyme of bovine origin. Arch Biochem Biophys 111:593–602 (1965).
99. Dohn DR, Anders MW. Assay of cysteine conjugate β-lyase activity with *S*-(2-benzothiazolyl)cysteine as the substrate. Anal Biochem 120:379–386 (1982).
100. Stevens JL. Isolation and characterization of a rat liver enzyme with both cysteine conjugate β-lyase and kynureninase activity. J Biol Chem 260:7945–7950 (1985).
101. Stevens J, Jakoby WB. Cysteine conjugate β-lyase. Mol Pharmacol 23:761–765 (1983).
102. Tateishi M, Suzuki S, Shimizu H. Cysteine conjugate β-lyase in rat liver: a novel enzyme catalyzing formation of thiol-containing metabolites of drugs. J Biol Chem 253:8854–8859 (1978).
103. Tomisawa H, Ichihara S, Fukazawa H, Ichimoto N, Tateishi M, Yamamoto I. Purification and characterization of human hepatic cysteine conjugate β-lyase. Biochem J 235:569–575 (1986).
104. Larsen GL, Stevens JL. Cysteine conjugate β-lyase in the gastrointestinal bacterium *Eubacterium limosum*. Mol Pharmacol 29:97–103 (1986).
105. Tomisawa H, Suzuki S, Ichihara S, Fukazawa H, Tateishi M. Purification and characterization of C-S lyase from *Fusobacterium varium*: A C-S cleavage enzyme of cysteine conjugates and some S-containing amino acids. J Biol Chem 259:2588–2593 (1984).
106. Alberati-Giani D, Malherbe P, Köhler C, Lang G, Kiefer V, Lahm H-W, Cesura AM. Cloning and characterization of a soluble kynurenine aminotransferase from rat brain: identity with kidney cysteine conjugate β-lyase. J Neurochem 64:1448–1455 (1995).
107. Malherbe P, Alberati-Giani D, Köhler C, Cesura AM. Identification of a mitochondrial form of kynurenine aminotransferase/glutamine transaminase K from rat brain. FEBS Lett 367:141–144 (1995).
108. Stevens JL. Cysteine conjugate β-lyase activities in rat kidney cortex: subcellular localization and relationship to the hepatic enzyme. Biochem Biophys Res Commun 129:499–504 (1985).
109. Abraham DG, Cooper AJL. Glutamine transaminase K and cysteine *S*-conjugate β-lyase activity stains. Anal Biochem 197:421–427 (1991).
110. Elfarra AA, Lash LH, Anders MW. α-Ketoacids stimulate rat renal cysteine conjugate β-lyase activity and potentiate the cytotoxicity of *S*-(1,2-dichlorovinyl)-L-cysteine. Mol Pharmacol 31:208–212 (1987).
111. Jones TW, Qin C, Schaeffer VH, Stevens JL. Immunohistochemical localization of glutamine transaminase K, a rat kidney cysteine conjugate β-lyase, and the relationship to the segment specificity of cysteine conjugate nephrotoxicity. Mol Pharmacol 34:621–627 (1988).
112. Lash LH, Elfarra AA, Anders MW. Renal cysteine conjugate β-lyase: bioactivation of nephrotoxic cysteine *S*-conjugates in mitochondrial outer membrane. J Biol Chem 261:5930–5935 (1986).
113. Lash LH, Nelson RM, Van Dyke RA, Anders MW. Purification and characterization of human kidney cysteine conjugate β-lyase activity. Drug Metab Dispos 18:50–54 (1990).
114. Perry SJ, Schofield MA, MacFarlane M, Lock EA, King LJ, Gibson GG, Goldfarb PS. Isolation and expression of a cDNA coding for rat kidney cytosolic cysteine conjugate β-lyase. Mol Pharmacol 43:660–665 (1993).
115. Stevens JL, Robbins JD, Byrd RA. A purified cysteine conjugate β-lyase from rat kidney cytosol: requirement for an α-keto acid or an amino acid oxidase for activity and identity with soluble glutamine transaminase K. J Biol Chem 261:15529–15537 (1986).
116. Stevens JL, Ayoubi N, Robbins JD. The role of mitochondrial matrix enzymes in the metabolism and toxicity of cysteine conjugates. J Biol Chem 263:3395–3401 (1988).
117. Abraham DG, Thomas RJ, Cooper AJL. Glutamine transaminase K is not a major cysteine S-conjugate β-lyase of rat kidney mitochondria: evidence that a high-molecular weight enzyme fulfills this role. Mol Pharmacol 48:855–860 (1995).
118. Abraham DG, Patel PP, Cooper AJL. Isolation from rat kidney of a cytosolic high molecular weight cysteine *S*-conjugate β-lyase with activity toward leukotriene E_4. J Biol Chem 270:180–188 (1995).
119. Dekant W, Berthold K, Vamvakas S, Henschler D, Anders MW. Thioacylating intermediates as metabolites of *S*-(1,2-dichlorovinyl)-L-cysteine and *S*-(1,2,2-trichlorovinyl)-L-cysteine formed by cysteine conjugate β-lyase. Chem Res Toxicol 1:175–178 (1988).
120. Dekant W, Lash LH, Anders MW. Bioactivation of the cytotoxic and nephrotoxic *S*-conjugate *S*-(2-chloro-1,1,2-trifluoroethyl)-L-cysteine. Proc Natl Acad Sci USA 84:7443–7447 (1987).
121. Dekant W, Urban G, Görsmann C, Anders MW. Thioketene formation from α-haloalkenyl 2-nitrophenyl disulfides: models for biological reactive intermediates of cytotoxic cysteine *S*-conjugates. J Am Chem Soc 113:5120–5122 (1991).
122. Eyre RJ, Stevens DK, Parker JC, Bull RJ. Renal activation of trichloroethene and *S*-(1,2-dichlorovinyl)-L-cysteine and cell proliferative responses in the kidneys of F344 rats and B6C3F1 mice. J Toxicol Environ Health 46:465–481 (1995).
123. Eyre RJ, Stevens DK, Parker JC, Bull RJ. Acid-labile adducts to protein can be used as indicators of the cysteine *S*-conjugate pathway of trichloroethene metabolism. J Toxicol Environ Health 46:443–464 (1995).
124. MacFarlane M, Schofield M, Parker N, Roelandt L, David M, Lock EA, King LJ, Goldfarb PS, Gibson GG. Dose-dependent induction or depression of cysteine conjugate β-lyase in rat kidney by *N*-acetyl-*S*-(1,2,3,4,4-pentachloro-1,3-butadienyl)-L-cysteine. Toxicology 77:133–144 (1993).
125. Iyer RA, Frink EJ Jr, Ebert TJ, Anders MW. Cysteine conjugate β-lyase-dependent metabolism of compound A (2-[fluoromethoxy]-1,1,3,3,3-pentafluoro-1-propene) in human subjects anesthetized with sevoflurane and in rats given compound A. Anesthesiology 88:611–618 (1998).
126. Lash LH, Elfarra AA, Rakiewicz-Nemeth D, Anders MW. Bioactivation mechanism of cytotoxic homocysteine *S*-conjugates. Arch Biochem Biophys 276:322–330 (1990).
127. Stevens JL, Hatzinger PB, Hayden PJ. Quantitation of multiple pathways for the metabolism of nephrotoxic cysteine conjugates using selective inhibitors of L-α-hydroxy acid oxidase (L-amino acid oxidase) and cysteine conjugate β-lyase. Drug Metab Dispos 17:297–303 (1989).
128. Sausen PJ, Elfarra AA. Cysteine conjugate S-oxidase: characterization of a novel enzymatic activity in rat hepatic and renal microsomes. J Biol Chem 265:6139–6145 (1990).
129. Sausen PJ, Duescher RJ, Elfarra AA. Further characterization and purification of the flavin-dependent *S*-benzyl-L-cysteine *S*-oxidase activities of rat liver and kidney microsomes. Mol Pharmacol 43:388–396 (1993).
130. Ripp SL, Overby LH, Philpot RM, Elfarra AA. Oxidation of cysteine *S*-conjugates by rabbit liver microsomes and cDNA-expressed flavin-containing monooxygenases: studies with *S*-(1,2-dichlorovinyl)-L-cysteine, *S*-(1,2,2-trichlorovinyl)-L-cysteine, *S*-allyl-L-cysteine, and *S*-benzyl-L-cysteine. Mol Pharmacol 51:507–515 (1997).
131. Sausen PJ, Elfarra AA. Reactivity of cysteine *S*-conjugate sulfoxides: Formation of *S*-[1-chloro-2-(*S*-glutathionyl)vinyl]-L-cysteine sulfoxide by the reaction of *S*-(1,2-dichlorovinyl)-L-cysteine sulfoxide with glutathione. Chem Res Toxicol 4:655–660 (1991).
132. Lash LH, Sausen PJ, Duescher RJ, Cooley AJ, Elfarra AA. Role of cysteine conjugate β-lyase and S-oxidase in nephrotoxicity: Studies with *S*-(1,2-dichlorovinyl)-L-cysteine and *S*-(1,2-dichlorovinyl)-L-cysteine sulfoxide. J Pharmacol Exp Ther 269:374–383 (1994).
133. Werner M, Birner G, Dekant W. Sulfoxidation of mercapturic acids derived from tri- and tetrachloroethene by cytochromes P450 3A: a bioactivation reaction in addition to deacetylation and cysteine conjugate β-lyase mediated cleavage. Chem Res Toxicol 9:41–49 (1996).
134. Bakke J, Gustafsson J-A. Mercapturic acid pathway metabolites of xenobiotics: generation of potentially toxic metabolites during enterohepatic circulation. Trends Pharmacol Sci 5:517–521 (1984).
135. Griffith OW, Meister A. Translocation of intracellular glutathione to membrane-bound γ-glutamyl transpeptidase as a discrete step in the γ-glutamyl cycle: glutathionuria after inhibition of transpeptidase. Proc Natl Acad Sci USA 76:268–272 (1979).
136. Inoue M, Morino Y. Direct evidence for the role of the membrane potential in glutathione transport by renal brush-border membrane vesicles. J Biol Chem 260:326–331 (1985).
137. Akerboom TPM, Narayanaswami V, Kunst M, Sies H. ATP-dependent *S*-(2,4-dinitrophenyl)glutathione transport in canalicular plasma membrane vesicles from rat liver. J Biol Chem 266:13147–13152 (1991).
138. Inoue M, Akerboom TPM, Sies H, Kinne R, Thao T, Arias IM. Biliary transport of glutathione *S*-conjugate by rat liver canalicular membrane vesicles. J Biol Chem 259:4998–5002 (1984).
139. Kobayashi K, Sogame Y, Hara H, Hayashi K. Mechanism of glutathione *S*-conjugate transport in canalicular and basolateral rat liver plasma membranes. J Biol Chem 265:7737–7741 (1990).
140. Niinuma K, Takenaka O, Horie T, Kobayashi K, Kato Y, Suzuki H, Sugiyama Y. Kinetic analysis of the primary active transport of conjugates metabolites across the bile canalicular membrane: Comparative study of *S*-(2,4-dinitrophenyl) glutathione and 6-hydroxy-5,7-dimethyl-2-methylamino-4-(3-pyridylmethyl) benzothiazole glucuronide. J Pharmacol Exp Ther 282:866–872 (1997).
141. Olive C, Board P. Glutathione *S*-conjugate transport by cultured human cells. Biochim Biophys Acta 1224:264–268 (1994).
142. Lash LH, Jones DP. Uptake of the glutathione conjugate *S*-(1,2-dichlorovinyl)glutathione by renal basal-lateral membrane vesicles and isolated kidney cells. Mol Pharmacol 28:278–282 (1985).
143. Lash LH, Jones DP. Transport of glutathione by renal basal-lateral membrane vesicles. Biochem Biophys Res Commun 112:55–60 (1983).
144. Lash LH, Jones DP. Renal glutathione transport: characteristics of the sodium-dependent system in the basal-lateral membrane. J Biol Chem 259:14508–14514 (1984).
145. Lash LH, Putt DA. Renal cellular transport of exogenous glutathione: heterogeneity at physiological and pharmacological concentrations. Biochem Pharmacol 58:897–907 (1999).
146. Simmons TW, Anders MW, Ballatori N. L-Cysteine and *S*-(1,2-dichlorovinyl)-L-cysteine transport in rat liver canalicular membrane vesicles: potential reabsorption mechanisms for biliary metabolites of glutathione and its *S*-conjugates. J Pharmacol Exp Ther 262:1182–1188 (1992).
147. Schaeffer VH, Stevens JL. Mechanism of transport for toxic cysteine conjugates in rat kidney cortex membrane vesicles. Mol Pharmacol 32:293–298 (1987).
148. Wright SH, Wunz TM, North J, Stevens JL. Na-Dependent transport of *S*-(1,2-dichlorovinyl)-L-cysteine by renal brush-border membrane vesicles. J Pharmacol Exp Ther 285:162–169 (1998).
149. Dantzler WH, Evans KK, Wright SH. Kinetics of interactions of para-aminohippurate, probenecid, cysteine conjugates and *N*-acetyl cysteine conjugates with basolateral organic anion transporter in isolated rabbit proximal renal tubules. J Pharmacol Exp Ther 272:663–672 (1998).
150. Lash LH, Anders MW. Uptake of nephrotoxic *S*-conjugates by isolated rat renal proximal tubular cells. J Pharmacol Exp Ther 248:531–537 (1989).
151. Lash LH, Xu Y, Elfarra AA, Duescher RJ, Parker JC. Glutathione-dependent metabolism of trichloroethylene in isolated liver and kidney cells of rats and its role in mitochondrial and cellular toxicity. Drug Metab Dispos 23:846–853 (1995).
152. Koob M, Dekant W. Metabolism of hexafluoropropene: evidence for bioactivation by glutathione conjugate formation in the kidney. Drug Metab Dispos 18:911–916 (1990).
153. Lash LH, Qian W, Putt DA, Jacobs K, Elfarra AA, Krause RJ, Parker JC. Glutathione conjugation of trichloroethylene in rats and mice: sex-, species-, and tissue-dependent differences. Drug Metab Dispos 26:12–19 (1998).
154. Green T, Dow J, Ellis MK, Foster JR, Odum J. The role of glutathione conjugation in the development of kidney tumours in rats exposed to trichloroethylene. Chem-Biol Interact 105:99–117 (1997).
155. Lash LH, Lipscomb JC, Putt DA, Parker JC. Glutathione conjugation of trichloroethylene in human liver and kidney: kinetics and individual variation. Drug Metab Dispos 27:351–359 (1999).
156. Hinchman CA, Ballatori N. Glutathione-degrading capacities of liver and kidney in different species. Biochem Pharmacol 40:1131–1135 (1990).
157. Green T, Odum J, Nash JA, Foster JR. Perchloroethylene-induced rat kidney tumors: an investigation of the mechanisms involved and their relevance to humans. Toxicol Appl Pharmacol 103:77–89 (1990).
158. Elfarra AA, Hwang IY. In vivo metabolites of *S*-(2-benzothiazolyl)-L-cysteine as markers of in vivo cysteine conjugate β-lyase and thiol glucuronosyl transferase activities. Drug Metab Dispos 18:917–922 (1990).
159. Lau SS, Kleiner HE, Monks TJ. Metabolism as a determinant of species susceptibility to 2,3,5-(triglutathion-*S*-yl)hydroquinone-mediated nephrotoxicity. Drug Metab Dispos 23:1136–1142 (1995).
160. Carlile DJ, Zomorodi K, Houston JB. Scaling factors to relate drug metabolic clearance in hepatic microsomes, isolated hepatocytes, and the intact liver. Drug Metab Dispos 25:903–911 (1997).
161. Kedderis GL. Extrapolation of in vitro enzyme induction data to humans in vivo. Chem-Biol Interact 107:109–121 (1997).
162. Brüning T, Lammert M, Kempkes M, Their R, Golka K, Bolt HM. Influence of polymorphisms of GSTM1 and GSTT1 for risk of renal cell cancer in workers with long-term high occupational exposure to trichloroethene. Arch Toxicol 71:596–599 (1997).
163. Sato A, Nakajima T, Fujiwara Y, Murayama N. A pharmacokinetic model to study the excretion of trichloroethylene and its metabolites after inhalation exposure. Br J Ind Med 34:55–63 (1977).
164. Clewell HJ III, Gentry PR, Gearhart JM, Allen BC, Covington TR, Andersen ME. Applying mechanistic information, pharmacokinetic modeling and margin of exposure evaluations in a novel risk assessment for trichloroethylene and its active carcinogenic metabolites: chloral hydrate, trichloroacetic acid,

dichloroacetic acid, and dichlorovinylcysteine. Document prepared for OSHA Directorate of Health Standards Programs and U.S. Environmental Protection Agency Office of Health and Environmental Assessment, 1995.
165. Lipscomb JC, Mahle DA, Butler GW, Brashear WT. Unpublished data.
166. Banki K, Elfarra AA, Lash LH, Anders MW. Metabolism of *S*-(2-chloro-1,1,2-trifluoroethyl)-L-cysteine to hydrogen sulfide and the role of hydrogen sulfide in *S*-(2-chloro-1,1,2-trifluoroethyl)-L-cysteine-induced mitochondrial toxicity. Biochem Biophys Res Commun 138:707–713 (1985).
167. MacFarlane M, Foster JR, Gibson GG, King LJ, Lock EA. Cysteine conjugate β-lyase of rat kidney cytosol: characterization, immunocytochemical localization, and correlation with hexachlorobutadiene nephrotoxicity. Toxicol Appl Pharmacol 98:185–197 (1989).
168. Birner G, Richling C, Henschler D, Anders MW, Dekant W. Metabolism of tetrachloroethene in rats: identification of N^{ε}-(dichloroacetyl)-L-lysine and N^{ε}-(trichloroacetyl)-L-lysine as protein adducts. Chem Res Toxicol 7:724–732 (1994).